Clinicopathologic comparison of patients with angiosarcoma involving just the eyelid versus patients with tumors involving the eyelid and other structures

	Eyelid	Eyelid and other structures	Wilson-Jones Angiosarcoma (Holden 1987)
number of patients	12	28	74
presentation	rapid	varriable	scalp/face
clinical	50% nodular	varriable	bruise-like macule
ulceration	0%	rarely	14%
misdiagnosed	25%	rarely	rarely
metastasis	0%	21%	23%
survival	100% at 3.2 years	43% dead at 3.3 years	50% died in 15 months
regression	1/16	0%	1/72
treatment	excision	68% surgery, 32% non-surgical	radiation
progression	rare	68%	frequent
Size	2.08 cm	5.0 cm	varriable

Conclusions: Patients with isolated eyelid angiosarcoma present at similar ages to patients with more extensive disease, their tumors rarely progress outward to involve extra-palpebral structures, and they do better with more conservative surgical-oncogical management when compared to patients with eyelid involvement secondary to more extensive face disease.

1711 Systemic IgG4 Disease and Orbital Inflammatory Lesions Including Necrobiotic Xanthogranuloma

K Singh, CG Eberhart. Brown University, Providence, RI; Johns Hopkins Hospital, Baltimore, MD.

Background: IgG4 disease is characterized by mass-forming lesions due to lymphoplasmacytic infiltrates rich in IgG4+ plasma cells with associated sclerosis and a raised serum IgG4 level. Systemic IgG4 disease related orbital inflammatory lesions are rare and poorly understood. We recently encountered a case of orbital necrobiotic xanthogranuloma(NXG) associated with confirmed systemic IgG4 disease. We analyzed the number of IgG4-positive plasma cells in this and an additional 16 orbital inflammatory lesions.

Design: Immunohistochemistry for IgG (polyclonal rabbit anti-human IGG, DAKO) and IgG4 (monoclonal mouse anti-human IGG4, ZYMED laboratories) was performed on formalin fixed, paraffin-embedded sections using standard techniques. IgG and IgG4 positive plasma cells were counted in random (maximum ten) high power fields (40X objective with 10X eyepiece).

Results: The table below summarizes our results for the 17 cases included in the study. The NXG(Figure1) in the confirmed case of systemic IgG4 disease had 119 IgG4 positive plasma cell per HPF (range 83 to 170) with a 55% mean percentage of IgG4 positive plasma cells (range 30% to 84%). The IgG4 positive plasma cell percentages in all other orbital inflammatory lesions were low and only one case of non-specific chronic dacryoadenitis with some sclerosis had 33 % IgG4 positive plasma cells in a single focus.

Diagnosis	Age(range)	M:F	IgG4+ plasma cells/HPF(mean, range)	IgG+ plasma cells /HPF(mean , range)	IgG4/IgG Plasma cell %(mean , range)
Necrobiotic xanthogranuloma(n=2)	62-67	1:1	63(0-170)	191(82-367)	30(0-84)
Chronic non-specific dacryoadenitis(n=10)	15-62	1:4	3(0-50)	56(1-241)	3(0-33)
Pseudotumor(n=4)	12-75	1:3	1(0-11)	35(9-112)	1(0-8)
Fungal infection(n=1)	80	F	1(0-4)	61(26-85)	2(0-5)

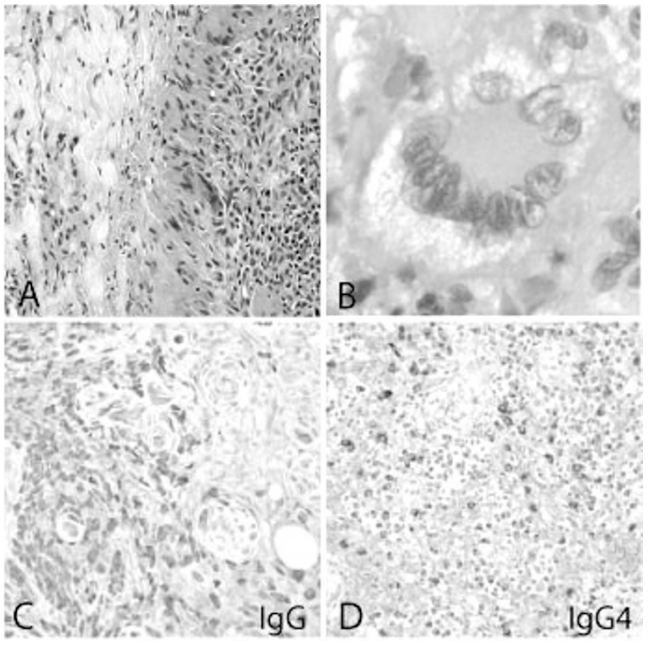

Conclusions: The chronic orbital inflammation cases we analyzed lacking sclerosis or a clear association to systemic IgG4 disease did not show an increase in IgG4 posiitve plasma cells. We conclude that IgG4-positive plasma cell percentages over 30% are uncommon in most orbital inflammatory lesions. We also extend the range of orbital lesions associated with systemic IgG4 disease to include NXG.

1712 Expression of c-KIT by Cell Morphology in Uveal Melanomas

P Tranchida, H Budev, S Sethi, H Jaratli, W Sakr, T Giorgadze. Wayne State University, Detroit, MI.

Background: Uveal melanoma (UM) is the most common primary intraocular cancer in adults. The overall prognosis is unfavorable, with 40-50% of patients developing metastases within 10 years of diagnosis. Recent reports showed that tyrosine kinase inhibitors (TKI) reduce growth in UM-derived cell lines and may be useful in treatment of patients with UM. However, data regarding c-KIT (tyrosine kinase receptor) expression in UM are rare and inconsistent. Our objective was to determine c-KIT immunohistochemical (IHC) expression in UM and correlate the staining patterns with tumor cell types according to modified Callender's classification.

Design: 21 consecutive UM cases treated by enucleation were retrieved (9 females, 12 males; age range: 33-83 years). Immunostaining for c-KIT was performed in representative tissue sections. The staining (cytoplasmic or membranous) was evaluated as negative (<10%), weak (10-50%), or strong (>50%).

Results: The table shows that c-KIT immunoreactivity correlated strongly with the cellular composition of UM. Strong IHC staining was prevalent in spindle cells (both A and B types) and in the spindle cell component of the mixed spindle and epithelioid morphology. Negative or weak IHC expression was evident in all cases of epithelioid UM and the epithelioid component of tumors with mixed morphology. Furthermore, c-KIT staining helped unveil areas with epithelioid morphology in the original H&E sections.

Results of c-KIT immunostaining

Case number	Tumor composition	c-KIT staining (spindle cell)	c-KIT staining (epithelioid)
1	mixed (SB>E)	strong	negative
2	SB	strong	NA
3	SB>SA	strong	NA
4	mixed (SB>SA>E)	strong	negative
5	SA>SB	strong	NA
6	SB	weak	NA
7	mixed (E>SB)	weak	weak
8	SB>SA	strong	NA
9	mixed (E>SB)	strong	negative
10	mixed (E>SB)	weak	negative
11	SB>SA	strong	NA
12	SB	strong	NA
13	mixed (SB>E)	strong	negative
14	SB	strong	NA
15	SB>SA	strong	NA
16	SB	strong	NA
17	mixed (SB>E)	strong	negative
18	SB	negative	NA
19	SB	strong	NA
20	SB	strong	NA
21	E	NA	negative

KEY: E=epithelioid, SA=spindle A, SB=spindle B, NA=Not applicable

Conclusions: Our results show that c-KIT immunoexpression is prevalent in spindle cell UM to the exclusion of purely or predominantly epithelioid tumors. These observations may provide a rationale for considering targeting therapy with TKI only in patients with UM of pure spindle cell type or mixed UM with predominance of spindle cells.

Pathobiology

1713 3'-End Sequencing for Expression Quantification (3SEQ) from Archival Tumor Samples

AH Beck, Z Weng, DM Witten, S Zhu, JW Foley, P Lacroute, CL Smith, R Tibshirani, M van de Rijn, A Sidow, RB West. Stanford University Medical Center, Stanford.

Background: Gene expression microarrays are the most widely used technique for genome-wide expression profiling. However, microarrays do not perform well on formalin fixed paraffin embedded tissue (FFPET). Consequently, microarrays cannot be effectively utilized to perform gene expression profiling on the vast majority of archival tumor samples.

Design: To address this limitation of gene expression microarrays, we designed a novel procedure (3'-end sequencing for expression quantification (3SEQ)) for gene expression profiling from FFPET using next-generation sequencing. We performed gene expression profiling by 3SEQ and microarray on both frozen tissue and FFPET from two soft tissue tumors (desmoid type fibromatosis (DTF) and solitary fibrous tumor (SFT)) (total n = 23).

Results: Analysis of 3SEQ data revealed many genes differentially expressed between the tumor types (FDR < 0.01) on both the frozen tissue (~9.6K genes) and FFPET (~8.1K genes). Analysis of microarray data from frozen tissue revealed fewer differentially expressed genes (4.64K), and analysis of microarray data on FFPET revealed very few (69) differentially expressed genes. Functional gene set analysis of 3SEQ data from both frozen tissue and FFPET identified biological pathways known to be important in DTF and SFT pathogenesis and suggested several additional candidate oncogenic pathways in these tumors.

Conclusions: These findings demonstrate that 3SEQ is an effective technique for gene expression profiling from archival tumor samples and may facilitate significant advances in translational cancer research.

1714 *Trim3*, the Human Homolog of *Drosophila Brain Tumor*, Regulates Neural Differentiation, c-Myc Expression and Glioma Growth Properties

DJ Brat, G Chen, F Rahman, Y Rong, C Tucker-Burden, C Hadjipanayis, EG Van Meir. Emory University School of Medicine, Atlanta, GA.

Background: Glioblastoma (GBM) is the most common malignant brain tumor. A CD133+ stem cell compartment has been described, yet its specialized properties are not

fully understood. *Drosophila Brain tumor (brat)* directs asymmetric neuroblast division and guides neural differentiation in the developing fly brain at least partially through its suppression of Myc. *Brat* mutation results in a massively enlarged brain consisting of neuroblasts with neoplastic properties. We investigated the role of *brat* homologs in directing zebrafish neural differentiation and in human GBMs for a potential role in modulating c-Myc and growth properties.

Design: Morpholino oligos directed at the zebrafish homolog of *brat, Trim3b,* were injected into single cell embryos. In situ hybridization and electron microscopy were used to characterize the resulting CNS phenotype. The human homolog of *brat*, *Trim3*, was studied in GBM cell lines, neurosphere cultures and GBM specimens by RT-PCR and Western blot. Transient transfection and lenitviral infection of *Trim3* expression constructs and shRNAs were used to study effects on c-Myc expression and glioma growth.

Results: Knock-down of *Trim3b* in zebrafish resulted in an enlarged head, reduced cell numbers and an enrichment of neuroblastic cells lacking differentiation. Using transgenic GFAP-GFP and Hu-GFP zebrafish, we found a marked reduction in the expression of these differentiation markers in *Trim3b* morpholino-treated fish. The stem cell marker *Notch1a* was slightly reduced in treated fish, consistent with lower cell numbers. The human homolog of *brat*, *Trim3* (11p15.5)*,* shows allelic loss in 25-30% of GBMs. We found that *Trim3* mRNA and protein expression were reduced in human GBM cell lines and specimens compared to astrocytes and normal brain, respectively. Overexpression of *Trim3* in human GBM cell lines led to reduced c-Myc protein and Myc target gene expression. This inverse relationship between Trim3 and c-Myc also held in GBM samples. Lentiviral infection of GBM cell lines with *Trim3* expression constructs led to reduced proliferation and colony formation in soft agar.

Conclusions: We suggest that the reduced Trim3 expression noted in human GBMs results in upregulated c-Myc, which could potentially enrich the stem cell compartment and enhance growth properties.

1715 Differential Expression Patterns of the Heterochromatin Proteins HP1α and HP1β in Different Tumor Types

A Contreras, MC Gutierrez, TK Hale. Baylor College of Medicine, Houston, TX; Massey University, Palmerston North, Manawatu-Wanganui, New Zealand.

Background: Heterochromatin are condensed regions in the genome with repressed transcription. HP1α and HP1β are two heterochromatin associated proteins that have been shown to be lost in various tumors. We have previously shown that HP1β is significantly decreased in thyroid follicular, papillary, and anaplastic carcinomas when compared to normal. In order to extend these studies, we performed Western blot analysis on thyroid papillary carcinomas and IHC on a tissue microarray with different tumor types.

Design: Frozen matched thyroid normal and papillary carcinoma tissue from 4 patients was obtained from the Christchurch Cancer Society Tissue Bank. Total protein was isolated from these tissue samples, resolved by SDS-PAGE, then transferred to nitrocellulose. The blots were then incubated with either a HP1α or HP1β antibodies. A Tissue Microarray (TMA) with 6 brain, 8 colon, 10 lung, 5 cervical, 10 uterine, 8 bladder, 9 breast, 10 ovarian, 10 prostate, and 6 kidney tumors was created. IHC using antibodies against HP1α and HP1β was performed on this TMA, and the presence of these proteins was analyzed.

Results: As shown below, both HP1α and HP1β are downregulated in thyroid papillary carcinomas when compared to normal. Interestingly, both proteins were lost to a greater degree in the 3 out of 4 cases with metastatic tumor (cases 1, 3, and 4).

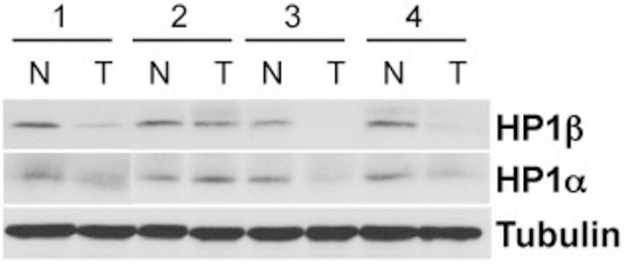

HP1α and HP1β were similarly expressed in the following tumors: brain, cervical, bladder, breast, ovarian, and prostate. In colon (7/8), lung (8/10), uterine (6/10), and kidney (6/6), HP1β is lost whereas HP1α expression is retained in a significant majority of these tumor types.

Conclusions: HP1α and HP1β is significantly decreased in thyroid papillary carcinoma when analyzed by Western blot. Thus, in thyroid carcinomas, loss of the HP1 proteins may result in altered gene expression that promotes tumorigenesis. A significant loss of these proteins may confer a metastatic advantage to this tumor type. Interestingly, the observation that HP1β is lost in a subset of tumors that retain HP1α expression may imply a different pathogenesis of these tumor types.

1716 Temporal Assessment of Host Response to Acellular Dermal Matrices

SS Daniel, G Henry, AN Husain. University of Chicago, Chicago, IL.

Background: Acellular dermal matrices (ADMs), such as Alloderm, are commonly used for soft tissue reconstruction. These products are derived from human cadaveric skin after a freeze-drying process, resulting in a collagen biomaterial. ADMs provide a biocompatible matrix useful for soft tissue replacement instead of polypropylene mesh, which has been shown to increase complication rates in some patients. Animal studies have demonstrated that biomaterials become revascularized accounting for its clinical success but, histologic examination in patients has not been extensively studied. The purpose of this study was to characterize the host cell invasion into ADMs, in patients, over an extended period of time.

Design: We prospectively identified 24 patients undergoing reconstructive surgery requiring use or revision of ADMs from 2007-2009. Two scar revisions specimens without use of ADMs and one ADM prior to implantation were used as controls. Sites of implantation included abdomen, breast and forearm. The duration of matrix implantation ranged from 2-10 months. Nine representative specimens from 4 patients were selected for trichrome, elastin, CD31 and smooth muscle actin (SMA) stains.

Results: Results are summarized in Table 1. Trichrome staining demonstrated thick collagen bundles in all ADMs. Elastic fibers were present between collagen bundles in the preimplantation specimen as well as the 3 month specimen, however, were absent in the 2, 5, 7 and 10 month specimens. CD31 demonstrated increasing vascularity of the specimens with longer implantation times. Fibroblasts were absent from pre-implantation ADM, but were identified in all implanted specimens. Myofibroblasts were not demonstrated by SMA staining.

Engraftment period	Immune response	Trichrome	Elastic	Vessels/hpf (CD31)
Control	Absent	Thin collagen bundles	Absent	4-7
Pre-implantation	Absent	Thick collagen bundles	Present	0
2 months	Absent within graft	Thick collagen bundles	Absent	2-5
3 months	Absent within graft	Thick collagen bundles	Present	5-9
5 months	Absent within graft	Thick collagen bundles	Absent	6-10
7 months	Absent within graft	Thick collagen bundles	Absent	6-8
10 months	Absent within graft	Thick collagen bundles	Absent	10-14

Conclusions: Analysis of ADMs demonstrated progressive fibroblast infiltration and vascular density without eliciting an immune response such as foreign body giant cell reaction.

1717 Ulcerative Colitis-Induced Carcinoma Development in NADPH-Oxidase GP91 Knock-Out Mice

P Dhakras, J Liao, AL Yang, GY Yang. Northwestern University, Chicago, IL.

Background: GP91^{phox} is the catalytic domain of the leukocyte NADPH oxidase responsible for superoxide production. Superoxide can cause DNA damage either by itself or by combining with NO to form the highly reactive species peroxynitrite, which may lead to mutation and genetic instability. In order to study the role of inflammation-caused oxidative stress in ulcerative colitis (UC)-induced colorectal carcinogenesis, the development of colorectal carcinoma was studied using the DSS-induced and iron-enhanced UC-carcinogenesis model in *gp91*$^{-/-}$deficient mice.

Design: Female wild-type C57BL/6 (*gp91*$^{+/+}$) and *gp91*$^{-/-}$ mice were administered 0.7% DSS (w/v) through the drinking fluid for 11 DSS cycles and fed 2-fold iron enriched diet.Swiss-rolled colonic specimens were collected and processed for histopathologic and immununohistopathologic analysis for inflammation, dysplasia and carcinoma.

Results: Colorectal inflammation and mucosal ulceration of mild severity were observed in both *gp91*$^{+/+}$ and *gp91*$^{-/-}$ mice. Twelve of 24 (50%) *gp91*$^{+/+}$ mice developed colorectal tumors after 11 DSS cycles treatment, with a tumor multiplicity of 1.12 0.17 (mean SE). In *gp91*$^{-/-}$ mice, significantly decreased tumor development was observed.Five of 21 (23.9%) mice developed colorectal tumors and the mean tumor number per *gp91*$^{-/-}$ mouse was 1.0 0.0. Histopathologically, the tumors were confirmed to be well-differentiated tubular and mucinous adenocarcinomas. Nitrotyrosine, an indicator of peroxynitrite-caused protein modification, was detectable by immunohistochemistry in inflammatory cells and epithelial cells of the colon in*gp91*$^{+/+}$ and *gp91*$^{-/-}$mice, and showed that there was significant decrease in staining intensity and number of nitrotyrosine-positive cells in *gp91*$^{-/-}$ mice.

Conclusions: These results suggest that the leukocyte NADPH oxidase(GP91^{phox}) is a key enzyme involved in inflammation-caused nitro-oxidative stress and carcinogenesis in this model system. These results provide important evidence on the relationship between inflammation, leukocyte NADPH oxidase, oxidative stress and carcinogenesis.

1718 A Unique TPA-Induced Trans-Membrane Protein Expression in Human Pancreatic Carcinoma Cells: A Novel Gene Involved in Pancreatic Cancer Growth through P42/44 MAPK

X Ding, MR Salabat, DJ Bentrem, MJ Strouch, RH Bell, TE Adrian, G-Y Yang. Northwestern University Feinberg School of Medicine, Chicago, IL.

Background: Pancreatic cancer is one of the most devastating human malignancies. Mechanisms for the uncontrolled pancreatic cancer growth are poorly understood. We have cloned a novel gene induced by tetradecanoylphorbol-acetate (TPA) in pancreatic cancer cells. The gene is located on human chromosome 3, and cloning of its full-length cDNA revealed that it encodes a putative transmembrane protein with 217 amino acids. In silico analysis suggested that the gene product is localized to the endoplasmic reticulum (ER), therefore, we named this gene product TPA-induced trans-membrane protein (TTMP). The current study was to investigate its expression profile, intracellular localization and modification, its role in pancreatic cancer growth and possible signal pathways involved.

Design: TTMP expression in human pancreatic adenocarcinoma, pancreatic cancer cell lines, immortalized pancreatic ductal cells and normal human tissue was determined by real time RT-PCR. TTMP cDNA was cloned into Lentiviral expression system. Intracellular localization and post-translation modification of TTMP was investigated by immunofluorescence microscopy and deglycoslytion. Effect of TTMP on cancer cell proliferation in vitro was determined by TTMP overexpression with lentivirus and downregulation with siRNA. SCID mice were used to evaluate effect of TTMP on tumor growth following Lentiviral transduction.

Results: TTMP is widely expressed in normal human tissues and is particularly abundant in pancreas. Decreased expression of TTMP was found in pancreatic carcinoma tissue (31 cases). The TTMP protein was localized to endoplasmic reticulum membrane and had post-translational N-glycosylation. Over-expression of TTMP suppressed pancreatic cell proliferation and induced G1 phase arrest. Shut-down of the TTMP gene product by

siRNA enhanced tumor cell proliferation. By implanting TTMP lentiviral-transduced pancreatic cancer cells into SCID mice, we further confirmed the in vitro results that TTMP gene product inhibited pancreatic cancer growth. Furthermore, over-expression of TTMP significantly decreases P42/44 MAPK phosphorylation.
Conclusions: The TTMP is a glycosylated protein and localizes to ER. It is involved in regulation of pancreatic adenocarcinoma growth, possibly via the P42/44 MAPK pathway. Our results further suggest that TTMP is a novel tumor suppressor gene and plays important role in pancreatic carcinogenesis.

1719 Verrucous Carcinoma May Arise Via HPV-Dependent or HPV-Independent Routes That Are Not Predictable from p16^{INK4a} Immunostaining

ED Dulaney, MF Evans, CS Adamson, Z Peng, V Rajendran, K Cooper. University of Vermont/Fletcher Allen Health Care, Burlington, VT.
Background: Verrucous carcinoma (VC) is a rare subtype of squamous cell carcinoma with unique clinicopathologic features, occurring in oral, genital, perianal and occasionally cutaneous locations. Previous studies have yielded conflicting data on the prevalence of human papilloma virus (HPV) and the specific genotypes found in VC. In addition, these studies have been restricted to VC in one or two anatomic sites.
Design: Search of our pathology department's computerized database for VC diagnosed between May, 1978 and February, 2009 identified 10 cases available for analysis: 1 anal, 3 vulvar and 6 oral specimens. The polymerase chain reaction (PCR), chromogenic *in situ* hybridization (CISH), and immunohistochemistry (IHC) for p16^{INK4a} were combined to investigate HPV infections in these tumors.
Results: HPV DNA was detected in seven VCs (70%) by PCR, identifying HPV31 in 3 cases (2 oral, 1 vulvar), HPV16 in two cases (1 vulvar, 1 oral), and single cases of HPV6 (oral) and HPV11 (anal). HPV was detectable by CISH in 5 PCR-positive cases: 2 vulvar (1 HPV16, 1 HPV31 [punctate nuclear signals, integrated HPV]), 1 anal (HPV11, diffuse nuclear signals [episomal HPV]) and 2 oral (1 HPV16, 1 HPV31 [punctate nuclear signals, integrated HPV]). Three PCR/CISH-positive samples demonstrated p16 ^{INK4a} staining. Overall, p16 ^{INK4a} IHC correlated with PCR results in 5 cases (50%) and with CISH results in 5 cases (50%).
Conclusions: These data indicate that VC from diverse anatomic locations may arise via HPV-dependent or HPV-independent routes. The HPV route may involve high risk (16, 31) or low risk (6, 11) HPV subtypes. However, it is also possible that HPV may be incidental to VC etiology in the cases positive for HPV by PCR only. Staining for p16^{INK4a} does not appear to be a simple surrogate marker for HPV in VC.

1720 Gamma Tocopherol Reduces Aberrant Crypt Foci in Azoxymethane-Treated Fisher 344 Rats

T Giorgadze, G Axelson, S Whaley, M Brannon, W Stone, S Campbell. Wayne State University, Detroit, MI; East Tennessee State University, Johnson City, TN.
Background: Aberrant crypt foci (ACF) are early neoplastic (dysplastic) lesions that are important in understanding colonic carcinogenesis in carcinogen-treated animals. Recent studies have shown that y-Tocopherol (the most common of four Vitamin E isoforms in the typical American diet) may play unique role in preventing colon cancer. We examined effects of dietary γ-Tocopherol (γT) on development of colonic ACF in azoxymethane-treated (AOM) Fisher 344 Rats.
Design: The rats were treated with 2 doses of AOM (15 mg/kg weight) by intraperitoneal injection on weeks 2 and 3 following weaning (age 6 weeks). Three AOM-treated groups were studied (12 rats in each). Group 1 (G1) were fed with no γT addition to the diet, groups 2 (G2) and 3 (G3) were fed γT at 0.4 mg/day (30 IU, low dose) and 5.75 mg/day (400 IU, high dose), respectively, in a modified AIN-76A diet (no vitamin E added, corn oil stripped to remove exogenous vitamin E). Control rats with no AOM treatment were fed 0.4 mg/day γT. Animals were sacrificed at 16 weeks of age. Colons were cut open and stained fresh with methylene blue (0.2% in buffered saline) for 60 min. The mucosal surface was equally divided into proximal and distal segments. The number (#) of ACF and crypt multiplicity (<4 or >4 crypts per focus) were counted at 100x magnification in each colonic segment.
Results: There was no difference in growth rate (rat mass) between the groups. G1 (γT-deficient) and G3 (high dose γT fed) rats developed significantly higher number of ACF compared to low dose γT fed G2 rats ($p<0.001$). Table 1 shows number of ACF and multiplicity (AVG and STD) in each group.

Table 1

Groups	Total # of ACF	<4 crypts	>4 crypts
G1 (no γT)	33+/-5.2	18.9+/-3.4	15.8+/-6.22
G2 (30 IU γT)	18.9+/-4.1	10.5+/-8.3	8.3+/-4.1
G3 (400 IU γT)	46.1+/-8.6	26.1+/-9.8	20.7+/-7.8
Control	2+/-2.6	2+/-2.6	0

Interestingly, in all groups the average number of ACF was significantly higher in the distal (D) colon compared to the proximal (P). Average ACF ratio (D/P) were: 26.1/2.7 in G1; 23.0/4.1 in G2; 39.8/5.0 in G3. Between the groups, there was no significant difference in average number of the proximal colon ACF.
Conclusions: 1) There is dose-dependant response between the number of ACF and γT dosage. 2) Low dose γT addition to the daily diet has chemoprotective effect in colon carcinogenesis. 3) High dose dietary γT may be even more harmful than γT-deficiency.

1721 EZH2 Regulates Growth of Estrogen Receptor Negative Breast Carcinomas by Regulating BRCA1 Localization

ME Gonzalez, X Li, K Toy, M DuPrie, CG Kleer. University of Michigan.
Background: EZH2 is an oncogene essential to promote proliferation and capable to trigger neoplastic conversion in the breast. EZH2 is overexpressed in breast carcinomas with high propensity to metastasize. We have reported that EZH2 promotes proliferation of breast cancer through downregulation of BRCA1 protein, but the mechanism is unknown. BRCA1 shuttles between the cytoplasm and nucleus to maintain genomic stability. AKT1 up regulation disrupts BRCA1 function by altering its nuclear localization and inducing genomic instability. We hypothesize that EZH2 regulates nuclear-cytoplasmic shuttling of BRCA1 in breast cells through AKT1.
Design: We developed two cell culture models: an inducible EZH2 up regulation system in MCF10A benign mammary cells, and a lentivirus-mediated shRNA interference to inhibit EZH2 in two ER negative breast cancer cells, CAL51 and MDA-MB-231. The effects of EZH2 on in vitro and in vivo tumorigenicity were determined by Western blots, immunofluorescence, proliferation, FACS, and xenograft and transgenic mouse models.
Results: EZH2 knockdown in breast cancer cells decreased their *in vivo* tumorigenicity. EZH2 shRNA knockdown in CAL51 cells increased BRCA1 nuclear localization in early S phase, decreased cell growth by delaying cell cycle progression, and decreased tetraploidy. EZH2 overepression in MCF10A cells decreased BRCA1 nuclear localization, increased proliferation and caused mitotic spindle defects and tetraploidy. EZH2 overepression increased total and phoshporylated AKT1 at serine 473. Specific pharmacologic inhibition of AKT reverted the effect of EZH2 on BRCA1 nuclear localization, proliferation, mitotic defects and tetraploidy. We also found that EZH2 directly interacts with AKT1 protein. Mammary glands of EZH2 trasnsgenic mice show up-regulation of AKT1 and a decreased in nuclear BRCA1 protein compared to wild type mice.
Conclusions: EZH2 inhibition decreases growth of ER negative breast cancer in mice. EZH2 regulates the nuclear-cytoplasmic shuttling of BRCA1 protein and influences BRCA1 functions on proliferation, mitotic spindle control, and maintenance of genomic stability in benign breast cells and in breast cancer cells. The regulation of BRCA1 localization and function by EZH2 requires AKT.

1722 Lymphovascular Tumor Emboli Recapitulate an In Vitro Mammosphere Stem Cell Phenotype

CE Graham-Lamberts, AL Llewellyn, Y Ye, K Yearsley, SH Barsky. University of Nevada School of Medicine, Reno, NV; The Ohio State University College of Medicine, Columbus, OH; Nevada Cancer Institute, Las Vegas, NV.
Background: The existence of stem cells in human cancers has been inferred by clonality experiments and marker studies *in vitro* and clinical observations *in vivo* concerning tumor recurrences and emerging drug resistance. We have studied the existence of stem cells in a human model of inflammatory breast cancer, termed MARY-X, a model which forms spheroids which are similar to normal tissue stem cell-derived mammospheres. Comparing MARY-X with common non-IBC breast carcinoma and normal cell lines, we found specific embryonal stem cell markers within the MARY-X spheroids. RT-PCR analyses of MARY-X also revealed the expression of transcriptional determinants essential for the pluripotency and self-renewal of human embryonal stem cells. Since MARY-X spheroids, when injected into mice, form tumors with florid lymphovascular emboli, we wondered whether tumor emboli from actual human cancers also recapitulated a mammosphere stem cell phenotype.
Design: We carried out laser capture microdissection of tumor emboli in 100 cases of human breast cancer including cases of both infiltrating ductal as well as lobular cancer. We also carried out similar dissections of lymphovascular tumor emboli in 50 non-breast cancer cases which included 25 non-small cell lung cancers and 25 pancreatic ductal carcinomas and compared the emboli to areas of non-embolic invasive carcinoma.
Results: By both RT-PCR and IHC, lymphovascular emboli exhibited five-ten fold higher stem cell markers including Stellar, H19, Rex-1, Nestin, CD133 and Aldehyde Dehydrogenase 1 (ALDH1) as well as stem cell transcriptional determinants including OCT4, SOX2, and Nanog. In addition, stem cell signaling pathways specifically involved in self-renewal and pluripotency including Bmi-1, Hedgehog and Notch 3 were activated selectively within the lymphovascular tumor emboli. These observations held true irrespective of the adhesion status (presence or absence of E-cadherin) or organ-specific origin of the embolus.
Conclusions: Our findings indicate that the lymphovascular embolus is not simply a cellular fragment that detaches from the main tumor but rather represents a selection for a stem cell phenotype. This finding may explain the increased resistance of lymphovascular tumor emboli to chemotherapy and the decreased disease-free survival and poorer prognosis exhibited by patients with significant lymphovascular emboli.

1723 Expression of the VEGF/VEGFR2 Regulated Fatty Acid Binding Protein 4 (FABP4) in Endothelial Cells of Ovarian Carcinomas and Metastasis

K Gwin, E Lengyel, S Dogan, R Buell-Gutbrod. University of Chicago, Chicago, IL.
Background: FABP4 is a member of the FABP family consisting of nine highly conserved cytosolic proteins that are expressed in a tissue-specific manner. They play an important role in uptake and trafficking of intracellular fatty acids as well as in gene expression, cell proliferation and differentiation. FABP4 has been primarily regarded as an adipocyte- and macrophage specific protein, but there is mounting evidence that it is also a regulator of cell proliferation in certain types of endothelial cells. Recent studies suggest that this endothelial FABP4 expression is regulated by the VEGF (Vascular endothelial growth factor)/VEGFR2 pathway. We hypothesized that FABP4 also has a function in endothelial cells of vasculature supplying ovarian carcinoma and their omental metastases.
Design: Archival paraffin embedded material of 18 serous ovarian carcinomas with corresponding omental metastases were examined by IHC for the expression and localization of FABP4 in the vasculature. Staining was evaluated in the endothelial cells of the primary carcinoma, ovarian stroma, omental fat, desmoplastic tumor interface and omental metastatic tumor.
Results: The endothelial cells in vessels associated with the primary ovarian tumor and omental tumor metastases did not express FABP4 (18/18 cases). Strong cytoplasmic and nuclear expression of FABP4 was observed in endothelial cells of capillaries and small

veins in the ovarian stroma adjacent to the carcinoma as well as in the desmoplastic tumor interface of the omental metastases (18/18 cases).
Conclusions: Expression of FABP4 in endothelial cells was confined to capillaries and small veins, which is the main angiogenic component of the vasculature. Small vessels in the direct vicinity of the tumor stained for FABP4 while no vessels of any size associated with serous carcinoma or carcinoma metastasis expressed it. VEGF is the key regulator for angiogenesis under both physiologic and pathologic conditions, and FABP4 is a known target of the activated VEGF/VEGFR2 pathway. Our findings suggest that FABP4 might have an important role in the survival and proliferation of ovarian tumor cells as well as for successful metastatic growth by helping to provide the necessary microvascular supply via angiogenesis. This is of interest, as in addition to the already available VEGF-inhibitors, selective FABP4 inhibitors are currently investigated as treatment options.

1724 Reversible Epithelial to Mesenchymal Transition Is Associated with Acquired Resistance to Sunitinib in Patients with Renal Cell Carcinoma: Evidence from a Xenograft Study

HJ Hammers, HM Verheul, B Salumbides, R Sharma, R Pili, GJ Netto. Johns Hopkins University, Baltimore.
Background: Tyrosine kinase inhibitors (TKIs) targeting angiogenesis via inhibition of the vascular endothelial growth factor (VEGF) pathway have changed the medical management of metastatic renal cell carcinoma. While the treatment with TKIs have demonstrated clinical benefit these drugs will eventually fail. The potential mechanisms of resistance to TKIs are poorly understood.
Design: To address this question we obtained an excisional biopsy of a skin metastasis from patient with clear cell renal carcinoma who initially had a response on sunitinib and eventually progressed on therapy. Tumor segments were grafted subcutaneously in athymic nude mice. Established xenografts were treated with sunitinib. Tumor size, microvascular density and pericyte coverage were determined. Plasma as well as tissue levels for sunitinib were assessed. A tumor derived cell line was established and assessed in vitro for a potential direct antitumor effects of sunitinib.
Results: To our surprise, xenografts from the patient who progressed on sunitinib regained sensitivity to the drug. At a dose of 40 mg/kg sunitinib caused regression of the subcutaneous tumors. Histology showed a marked reduction in microvascular density and pericyte dysfunction. More interestingly, histological examination of the original skin metastasis revealed evidence of epithelial-to-mesenchymal transition while the xenografts showed reversion to the clear cell phenotype. In vitro studies showed no inhibitory effect on tumor cell growth at pharmacologically relevant concentrations.
Conclusions: The histological examination in this xenograft study suggests that reversible epithelial-to-mesenchymal transition may be associated with acquired tumor resistance to TKIs in patients with clear cell renal carcinoma.

1725 Mammalian Target of Rapamycin (mTOR) Regulates Cellular Proliferation and Tumor Growth in Urothelial Carcinoma

DE Hansel, E Platt, M Orloff, J Harwalker, S Sethu, JL Hicks, A De Marzo, R Steinle, E Hsi, D Theodorescu, C Eng. Cleveland Clinic, Cleveland, OH; Johns Hopkins Hospital, Baltimore, MD; University of Virginia, Charlottesville, VA.
Background: Mammalian target of rapamycin (mTOR) signaling has been associated with aggressive tumor growth in many cancer models, although its role in urothelial carcinoma (UCC) has not been explored in detail.
Design: We evaluated expression of phosphorylated mTOR (P-mTOR) and a downstream target, ribosomal S6 protein (P-S6), in 121 cases of UCC by immunohistochemical analysis. We next determined the effects of mTOR inhibition via rapamycin administration on cell proliferation in UCC cell lines RT4, T24, J82 and UMUC3, all of which expressed mTOR signaling components with the exception of PTEN in UMUC3 cells. Mouse studies were performed using T24-xenografted mice subjected to intraperitoneal vehicle (n=9) or 2.5 mg/kg rapamycin administration (n=9) twice weekly for 4 weeks to evaluate bladder tumor growth.
Results: Phosphorylated mTOR and phosphorylated S6 was identified in 74% (90/121) and 55% (66/121) of UCCs, respectively. P-mTOR intensity and %positive cells were associated with reduced disease-specific survival ($p=0.041$, $p=0.078$, respectively) and P-mTOR intensity corresponded to increased pathologic stage ($p<0.001$). Rapamycin treatment resulted in a dose-dependent reduction in proliferation to 12% of control and was significant at 1 nM in J82, T24 and RT4 cells ($p=0.002$, $p=0.002$, $p=0.03$, respectively) and at 10 nM in UMUC3 cells ($p=0.03$). Reduced proliferation corresponded with reduced P-S6 levels by western blot. Administration of rapamycin to T24-xenografted mice resulted in a 55% reduction in tumor volume ($p=0.03$) and a 40% reduction in proliferation index ($p<0.01$) as compared to vehicle-injected mice.
Conclusions: These findings indicate that mTOR pathway activation frequently occurs in UCC and that inhibition of this pathway suggests a potential means by which to reduce urothelial tumor cell growth.

1726 Blockade of CCN6 Activates Growth Factor-Independent Survival of Breast Cells through the Phosphatidylinositol 3-Kinase/Akt Pathway

W Huang, ME Gonzalez, K Toy, CG Kleer. University of Michigan, Ann Arbor, MI.
Background: CCN6 is a secreted cysteine rich matricellular protein (36.9 kDa) that modulates IGF-1 signaling in breast cells and exerts tumor suppressor functions in inflammatory breast cancers. CCN6 loss has been associated significantly with decreased breast cancer cell growth and proliferation, and with the development of metastasis. However, the details of the survival mechanism remain undefined.
Design: We developed shRNA knockdown of CCN6 using lentiviral vectors in two benign human mammary epithelial cells: HME and MCF10A. We studied cell proliferation in complete medium and under serum starvation by WST-1 and trypan blue assays. Apoptosis was studied using flow cytometry. Protein and mRNA expression were measured by Western blot and real time PCR. Anchorage independent growth was evaluated using soft agar, and anoikis (detachment-induced cell death) was investigated using poly-HEMA assays.
Results: We found that CCN6 blockade protects breast cells from apoptosis and activates growth factor-independent survival. In the absence of serum, CCN6 knockdown allowed MCF10A and HME cells to grow in anchorage independent conditions in soft agar and protected the cells from anoikis. Upon serum starvation, CCN6 knockdown in MCF10A and HME cells induced Akt phosphorylation at serine 473. Both cell survival and Akt phosphorylation were stunted in CCN6 knockdown cells when treated with either recombinant human CCN6 protein or the phosphatidylinositol 3-kinase inhibitor LY294002. We further identified that the survival and apoptotic effects of CCN6 knockdown were reverted by specific shRNA downregulation of Akt-1.
Conclusions: Our data show that CCN6 knockdown promotes anchorage independent growth, proliferation and resistance to detachment induced cell death (anoikis), all features of malignant conversion. Furthermore, we pinpoint one mechanism by which CCN6 controls survival of breast cells, implicating the PI3K/Akt-1 pathway.

1727 Expression Pattern of Argininosuccinate-Synthetase (ASS) in Normal and Tumor Tissue as a Marker for Susceptibility to Arginine-Deiminase (ADI) Therapy

A Jungbluth, J Tassello, D Frosina, N Hanson, G Ritter, BW Wu, LJ Old. Ludwig Institute for Cancer Research, New York, NY; Polaris Pharmaceuticals, San Diego, CA.
Background: Enzymatically induced amino acid deprivation of malignant tumors (e.g.asparaginase in acute leukemia) lacking particularly enzymes is a well established therapeutic concept for malignant disease. Arginine-Deiminase (ADI) treatment of tumors is based on a similar concept. Tumor cells lacking argininosuccinate synthetase (ASS) are arginine-auxotrophic and depend on extracellular arginine uptake. ADI treatment lowers blood arginine levels and tumor cell death is potentially induced by amino acid deprivation. However, little is know about the presence of ASS in normal and tumor tissues on the actual protein level.
Design: A monoclonal antibody (mAb) to ASS was generated employing ASS fusion protein and classical hybridoma technology. The novel reagent, mAb 195-21-1 was tested for specificity and its suitability in IHC. Subsequently, panels of normal organs and tumors were analyzed by IHC for presence of ASS.
Results: MAb 195-21-1 worked well in paraffin embedded tissue using heat-based antigen retrieval techniques. In normal tissues, ASS was widely distributed and present in most normal organs such as kidney, liver, lung, gastro-intestinal tract and others. endothelial cells were positive in vessels of all analyzed tissues. Interestingly, particular cells remained negative such as pancreatic islets, melanocytes, as well as adrenal medulla. In most analyzed tumors such as carcinomas of the lung, GIT, kidney and breast, as well as various sarcomas ASS was expressed ranging from 25%-100% ASS-positive tumor cells, though single tumors showed only focal ASS expression. However, in melanoma, neuroendocrine carcinomas and SCLC only ASS-expression was absent or present in only focal tumors cells.
Conclusions: ADI induces efficient lowering of peripheral arginine levels and tumor cells lacking ASS are potentially susceptible to ADI administration. In normal organs, ASS is widely distributed showing expression in most tissues. Its presence in tumors parallels its expression in normal tissue with colorectal, kidney and breast cancer being mostly ASS-positive though occasional neoplasms show little ASS expression. However, SCLC, melanomas, and neuroendocrine carcinomas show little to none ASS expression. Our study indicates that melanoma, small cell lung cancer, and neuroendocrine carcinomas are potential candidates for ADI-based cancer therapy.

1728 Mechanistic Investigation of the p16[INK4A] Pathway

L Kehoe, CD Spillane, M Gallagher, O Sheils, C Martin, JJ O'Leary. Trinity College Dublin, Dublin, Ireland; Coombe Women and Infants University Hospital, Dublin, Ireland.
Background: Unravelling effects of high risk HPV oncoproteins has led to the discovery of dysregulated proteins and potential biomarkers. One of these is p16[INK4A]. Although p16 protein expression is used diagnostically, little is known about its transcriptional regulation and cell cycle involvement.
Design: Using HaCaT, a p16 protein null cell line, we aimed to determine cause and effects of p16 up regulation in cervical cancer (CC). We also examined the expression profile of a naturally occurring transcript [ANRIL] in CC cell lines, CIN, cGIN squamous cell carcinoma (SCC) and adenocarcinoma.
Results: HaCaT cells have been reported p16 null due to promoter methylation. We have discovered HaCaTs are expressing p16 mRNA and its promoter is unmethylated. Western blots indicate lack of detectable protein expression. We hypothesise p16 is undergoing post transcriptional regulation (PTR) in HaCaT cells. This is possibly due to interference by RNA molecules such as natural anti-sense transcripts (NATs) and microRNAs (miRNA). Results show the presence of p16 message at the polysome. Though miR-24 has been described in PTR of p16, we did not find this effect in HaCaT cells. A large NAT [ANRIL], which overlaps p14/p15, may play a role in regulating the INK4A/ARF locus. This NAT can be detected in total and polysomal RNA from HaCaT, HeLa and C33A cells. Due to its large size, different regions were investigated. All were present in cell lines, indicating further processing of any of these regions to small RNAs is not a factor in p16 PTR in HaCaT. Evaluation of ANRIL in CC and pre-cancer found no significance on comparison to normal cervix in CIN1, CIN3 and adenocarcinoma. Over-expression of ANRIL was found in cGIN and SCC cases. This data indicates expression of the INK4A/ARF locus and its NAT [ANRIL] is uncoupled in CC. Comparative miRNA profiling of HaCaT p16 protein incompetent cells to p16 competent cell lines [both HPV positive and negative] revealed a panel of 26 miRNAs; possible regulators of p16 transcript.
Conclusions: Bypassing p16 cellular control is an important mechanism in cancer development. We have found p16 control in HaCaT cells is bypassed by preventing p16

protein expression, facilitating creation of the HaCaT immortal but non-tumourgenic phenotype. We have also shown expression of ANRIL and the INK4A/ARF locus is uncoupled in CC, indicating HPV induced p16 over-expression is autonomous in CC and pre-cancer confirming the dominant role of HPV E7 in this setting.

1729 Nanocurcumin Formulation Increases Bioavailability of Curcumin and Prevents Experimentally Induced Liver Fibrosis

M Khan, S Bisht, A Maitra, RA Anders. The Johns Hopkins School of Medicine, Baltimore, MD.

Background: Chronic liver disease is a leading cause of death worldwide. Liver fibrosis is a hallmark of chronic liver disease. There are few treatment options for preventing progressive chronic liver disease. The natural product curcumin is a polyphenol extract from the spice turmeric which has been shown to prevent liver fibrosis in mice. However, these studies are hampered by requiring ingestion of megadoses of curcumin which still results in poor bioavailability. We have developed a nanoparticle formulation of curcumin, nanocurcumin (NC), which is fully soluble in aquoues media. We wish to test if NC increases bioavailability of curcumin and can prevent liver fibrosis in mice.

Design: Pharmakokinetics: Two formulations, one of NC and the other of free curcumin (FC) in corn oil were administered through the intraperitoneal (i.p.) route as a single dose of 25mg/kg to 6 mice each. The level of curcumin in the blood was measured by HPLC at 1, 2, 4, 8, and 24 hours. **Fibrosis:** Mice (n=5-10/group) were treated with aqueous NC 25mg/kg or control i.p. injection every other day for 2 weeks. Carbon tetrachloride in oil or control oil was given twice /wk i.p. over 2 weeks. Liver tissue was harvested for sirus red staining, hydroxyproline (collagen) content and serum collected for alanine aminotransferase (ALT) enzymatic assay and TNFalpha ELISA.

Results: Pharmakokinetics: We found curcumin levels peaked in the serum at 5 hrs and persisted 20 hrs post NC injection, while FC was not detectable at all time points. No toxicities were noted. **Fibrosis:**

Effects of Nanocurcumin

Assay	Control	NC Treated
Sirus red	Bridging fibrosis	Portal fibrosis*
Hydroxyoproline	250 +/- 20	130 +/- 25*
Serm ALT	300 +/- 75	175 +/- 100*
Serum TNF alpha	120 +/- 35	non-detectable*

* stat significant

Conclusions: We found nanocurcumin delivery markedly raises the bioavailability of curcumin and is a potent liver antifibrotic agent which appears to work by inhibiting TNF alpha. Nanocurcumin is a promising formulation with therapeutic implications in treating chronic liver disease.

1730 PAX8 Is Highly Sensitive and Specific for Mullerian, Renal and Thyroid Neoplasms: A Study of 1500 Epithelial Tumors

AR Laury, JL Hornick, H Piao, R Perets, J Barletta, LR Chirieac, JF Krane, R Lis, M Loda, R Drapkin, MS Hirsch. Brigham and Womens Hospital, Boston, MA; Dana Farber Cancer Institute, Boston, MA.

Background: PAX8 is a paired homeobox gene critical for development of the thyroid and urogenital tract. Expression has been described in tumors of the kidney, thyroid and Mullerian tract, but a large study, including a wide variety of epithelial neoplasms from multiple organs, to address specificity has not been performed.

Design: PAX8 immunohistochemistry was performed, after pressure cooker antigen retrieval using a rabbit anti-PAX8 polyclonal antibody (Proteintech; 1:800) on formalin-fixed, paraffin embedded tissue from 1500 tumors retrieved from department files. These 1500 cases included 701 whole tissue sections and 799 tumors in tissue microarrays from multiple organs. Only nuclear staining was scored as positive. Western blot analysis with PAX8 was also performed on renal, ovarian, prostatic, breast, colonic, cervical, and brain tumor cell lines.

Results: Nuclear PAX8 staining was present in 94% (58/62) of thyroid tumors, 61% (95/155) of renal cell carcinomas, 80% (12/18) of oncocytomas, 99% (151/152) of high grade ovarian serous carcinomas, and 38% (58/152) of endometrial adenocarcinomas. Of the remaining 961 evaluated tumors, only 15 cases (1.6%) demonstrated weak or focal PAX8 positivity. These 15 cases included 3 bladder urothelial carcinomas, 4 lung squamous cell carcinomas, 2 esophageal adenocarcinomas, 1 pancreatic adenocarcinoma, 1 ovarian Sertoli-Leydig cell tumor, 3 testicular mixed germ cell tumors, and 1 acinic cell carcinoma. All 946 remaining tumors, including, but not limited to those from the prostate, colon, stomach, liver, adrenal gland, and head and neck, as well as small cell carcinomas from the lung, cervix, and ovary, were PAX8 negative. PAX8 specificity was confirmed by Western blot analysis, as expression was only detected in ovarian and renal cell carcinoma lines.

Conclusions: PAX8 is a highly sensitive marker for ovarian serous and thyroid carcinomas, but is also expressed in a significant proportion of renal and other Mullerian tumors. Importantly, all lung adenocarcinomas, breast and adrenal neoplasms, as well as the majority (148/151) of GI tumors were negative for PAX8. Therefore, strong PAX8 expression is excellent for confirming site of tumor origin. In a subset of cases, additional markers such as TTF-1, RCC, and WT-1 may be needed to distinguish among the 3 most common PAX8-positive tumors.

1731 Field Change in Bladder Carcinogenesis: The Concept of Forerunner Genes

S Lee, SK Lee, S Zhang, J Bondaruk, T Majewski, W Chung, L Xiao, C Guo, JP Issa, M Bar-Eli, K Baggerly, B Czerniak. The University of Texas M D Anderson Cancer Center, Houston, TX.

Background: Analysis of genomic imbalances can guide us to those chromosomal regions that contain genes playing a role in tumor development. In sporadic epithelial cancers that develop from microscopically recognizable *in situ* conditions the early events maybe deduced from the geographic relationship between genomic imbalance and precursor *in situ* conditions.

Design: Using whole-organ histologic and genetic mapping approach, we matched the clonal allelic losses in distinct chromosomal regions to specific phases of bladder neoplasia and produced a detailed genetic map of human bladder cancer development. The genetic changes mapped to six regions at 3q22–q24, 5q22–q31, 9q21–q22, 10q26, 13q14, and 17p13, which may be critical for the development of bladder cancer. In addition, we performed high-resolution mapping within one region on chromosome 13q14, containing the model tumor suppressor gene RB1, and defined a minimal deleted region associated with clonal expansion of *in situ* neoplasia. These analyses identified novel target genes, termed forerunner (FR) genes, involved in early phases of cancer development.

Results: The functional studies focused on the two nearest candidate FR genes flanking *RB1*. These were *ITM2B*, which encodes a mitochondrial membrane protein with a BH3 domain, and *CHC1L*, which encodes a GEF protein for the ras-related GTPase. Surprisingly, a third candidate FR gene, *P2RY5* was actually located within intron 17 of *RB1* and encodes a G-protein-coupled receptor. *ITM2B* and *P2RY5* modulated cell survival and were silenced by methylation or point mutations, respectively. We also showed that homozygous inactivation of *P2RY5* was antecedent to the loss of *RB1* during tumor development, and that nucleotide substitutions in *P2RY5* represent a cancer predisposing factor. Our recent studies of another candidate FR gene, ARL11 encoding ADP-ribosylation factor-like tumor suppressor protein 1, have identified an unexpected link between the recessive events in the 13q14 region and up-regulation of one of the most important oncogenic pathways, namely the ras signaling.

Conclusions: The FR genes represent a new class of genes mapping near critical model tumor suppressors, such as RB1, whose loss of function drives incipient clonal expansion of phenotypically normal cells facilitating the subsequent inactivation of tumor suppressors and malignant transformation.

1732 COMMD1 Is an Inhibitor of Intestinal Inflammation and Colitis in a Myeloid-Specific Knockout Mouse Model

H Li, SD Melton, C Komarck, X Mao, B van de Sluis, C Wijmenga, LW Klomp, RM Genta, E Burstein. UT Southwestern Medical Center, Dallas, TX; Univ. of Michigan Medical School, Ann Arbor, MI; Univ. of Groningen, Groningen, Netherlands; Utrecht University, Utrecht, Netherlands.

Background: Nuclear factor-kappa B (NF-κB) is a key transcriptional regulator of innate and adaptive immunity. NF-κB inhibition protects against chronic intestinal inflammation and necrotizing enterocolitis in animal models. The copper metabolism (Murr1) domain containing 1 gene (*COMMD1*) is a regulator of copper homeostasis, sodium uptake, and NF-κB. *COMMD1* functions as an inhibitor of NF-κB mediated gene expression, but its relative contribution to the control of inflammation has not been studied *in vivo* up to this point. This study examines the role of *Commd1* in intestinal inflammation and colitis in mice with myeloid-specific knockout of *Commd1*.

Design: Using the *LysM-Cre* transgene, twenty myeloid *Commd1*-deficient mice were generated by Cre-LoxP mediated recombination. Twenty six wild-type mice were studied as controls. Colitis was then induced using dextran sulfate sodium (DSS). The phenotypic effects were evaluated via disease activity index (DAI), colon length, and histopathology. The DAI included weight loss, rectal bleeding, and diarrhea. The histopathological score of colitis was derived by grading four categories (crypt loss, crypt distortion, inflammation, and hyperplastic epithelial changes) on a scale of 0-4.

Results: Loss of *Commd1* in myeloid cells significantly worsened the course of DSS-induced colitis.

Measurements of Colitis

	Wild-type	Commd1 Knockout	T-test (*p* value)
Number (n)	20	26	
DAI (au)	9.1	11.4	9.00 E-07
Weight (%)	85	77	7.00 E-06
Survival (%)	95	45	0.05
Colon length (cm)	6.1	5.5	0.002
Histolpathology score (au)	2.83	3.7	0.04

Conclusions: These studies show *Commd1* deficiency in the myeloid compartment of mice plays a significant role in the regulation of DSS-induced colitis. The regulation of *COMMD1* expression and/or function in patients with inflammatory bowel disease could play a role in the pathogenesis of inflammatory bowel disease, and perhaps offer a novel pathway for targeted therapeutics.

1733 An EGFR-Sox9 Signaling Cascade Links Urothelial Development, Regeneration, and Cancer

S Ling, X Chang, T Lee, L Marchionni, X He, BW Simons, Z Huang, D Sidransky, G Netto, DM Berman. Johns Hopkins Medical Institutions, Baltimore.

Background: Like many carcinomas, urothelial carcinoma (UrCa) is associated with chronic injury. This association is poorly understood, but could elucidate the etiology and treatment of this disease.

Design: Using western blot and immunohistochemistry, we investigated expression of the transcriptional regulator SRY-related HMG box 9 (SOX9), total and activated forms of Epidermal growth factor receptor (EGFR) and mitogen activated protein kinase (MAPK) proteins, as well as EGFR ligands in injured benign and malignant urothelial cells and tissue samples. Sox9 function was assayed for growth and invasion using human BFTC-905 UrCa cells transfected with scrambled (control) or specific short hairpin RNA expression vectors. A selection of both benign and malignant urothelial cell lines were cultured with EGFR and MAPK pathway agonists and antagonists, hydrogen peroxide, urea, and NaCl.

Results: We identified induction of the Sox9 in urothelial regeneration and in UrCa. In mouse bladder, Sox9 expression showed two spikes of increased expression -- first during embryonic growth and again during physiologic regeneration postnatally. In adults, and in cultured benign human urothelial cells, Sox9 protein was markedly

induced by a variety of injuries, including systemic administration of the carcinogen cyclophosphamide, culture with hydrogen peroxide, and osmotic stress. Sox9 is a known target of MAPK signaling, which also induced Sox9 in urothelial injury and resulted from upregulation of Heparin binding EGF-like growth factor (HB-EGF) and amphiregulin through EGFR. EGFR expression was highest in the urothelial basal layer, normally protected from urinary EGFR ligands by overlying superficial cells. With chronic breaches of urothelial integrity, EGFR-Sox9 stimulation may promote urothelial carcinogenesis, as Sox9 expression was significantly upregulated in invasive human UrCa samples (n=82) and cell lines. The EGFR-Sox9 signaling axis operated in UrCa cells and was required for cell migration and invasion.
Conclusions: These results identify a novel, potentially oncogenic signaling axis that links urothelial injury to UrCa. Inhibiting the operation of this pathway is possible through a variety of pharmacologic approaches and may play a role in prevention and treatment of UrCa.

1734 Raman Molecular Imaging: A Novel Technique for Histopathological Evaluation of Tissue Specimens

JS Maier, AJ Drauch, SD Stewart. ChemImage Corporation, Pittsburgh, PA.
Background: Raman Molecular Imaging (RMI) is a digital, non-destructive, reagentless tissue imaging approach based on Raman spectroscopy. RMI provides an image of a sample wherein the contrast derives from Raman scattering of light off of the constituent molecules of the tissue.
Design: Thin sections from formalin fixed, paraffin-embedded samples were obtained in standard fashion and applied to aluminum coated microsope slides. Digital Raman images were acquired using a FALCON™ Raman imaging system. After Raman imaging, samples were stained to facilitate histological correlation between traditional H&E and Raman imaging modalities. Digital images were created by process of constructing a reference library of spectra for selected histological types, and subsequent segmenting using spectral mixture resolution. Analysis included subjective comparison of Raman images to imagery of the stained sample.
Results: Images show good qualitative correlation between the reagentless RMI and the images of tissue stained in traditional fashion in terms of histological features including prostate epithelium and stroma, renal glomerular cells and tubular cells, and red blood cells.

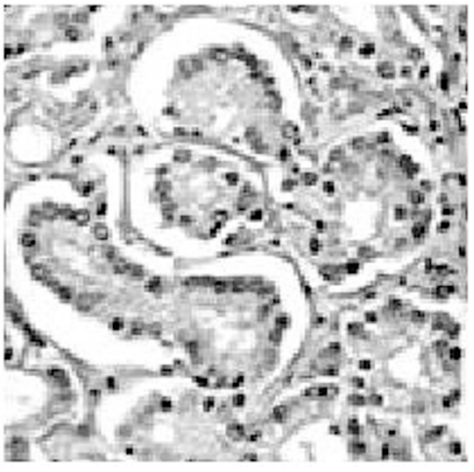

Figure 1 shows an H&E stained field of view from a prostate.

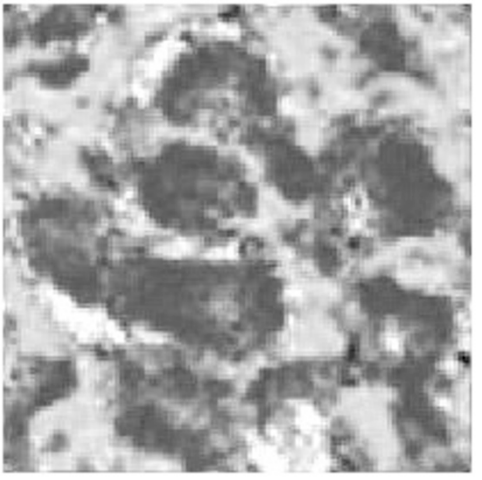

Figure 2 shows the image resulting from spectral mixture resolution applied to RMI of the same field of view of prostate prior to staining.
Conclusions: Raman Molecular Imaging (RMI) is a novel technique for digital image based analysis of unstained thin sections of tissue. RMI carries information about the molecular environment at the cellular and subcellular level in tissues as manifested by accurate histological sectioning based on comparison to existing, stain-based approaches. The molecular information at the basis of the contrast in RMI may have correlation with pathophysiology that is of clinical interest. Further study of RMI in application to clinical questions of interest is warranted.

1735 Clonal Relationship of Plasma Cells to Lymphoid Component in Mantle Cell Lymphoma with Monotypic Plasma Cells

JT Malik, et al. Multicenter Collaborative Study.
Background: The differentiation of B-cells into plasma cells is a well-defined process that is regulated by transcriptional factors. Plasma cell precursors are mostly derived from the germinal center (GC) or marginal zone cells, and terminally differentiate into plasma cells at various peripheral sites. Primary follicle and mantle-zone B-cells are composed of naive, quiescent B-cells which rarely mature into plasma cells. These findings are reflected in B-cell lymphomas by the observations that while lymphomas arising from GC or post-GC B-cells often exhibit plasmacytic differentiation, this is a rare finding in lymphomas arising from pre-GC naive B-cells.
Design: Eight cases of mantle cell lymphoma (MCL) with monotypic plasma cell populations are identified from 6 medical centers. In each of these cases, the MCL cells and the plasma cells are evaluated by immunohistochemistry, fluorescence in situ hybridization (FISH), and Fluorescence immunophenotyping and Interphase Cytogenetics as a Tool for the Investigation of Neoplasms (FICTION) analysis.
Results: Three cases reveal typical morphologic and immunohistochemical features of MCL, but also contain small foci of plasma cells with identical monotypic immunoglobulin light chain expression. FICTION analysis demonstrates the characteristic t(11;14)(q13;q32) in the MCL cells and plasma cells in two of these three cases. Two cases are composed predominantly of clonal plasma cells with different immunoglobulin light chain expression. FICTION analysis demonstrates the t(11;14)(q13;q32) in the smaller population of MCL cells, but not in the larger population of plasma cells. One case is composed of MCL cells as well as smaller, monotypic plasma cell and non-MCL lymphoid components. FICTION analysis in this case, using light chain and CD138, demonstrates the t(11;14)(q13;q32) in the MCL cells but not in the plasma cells. FICTION analysis failed in two of the cases.
Conclusions: Our findings suggest that clonal monotypic plasma cells may accompany MCL cells. Immunohistochemical and molecular studies demonstrate that in two out of eight cases the MCL cells and plasma cells are derived from the same neoplastic B-cell clone. In four cases the plasma cells may represent a composite lymphoma of MCL and extramedullary plasmacytoma or plasmacytoma-like marginal zone lymphoma. FICTION analysis failed in two cases. Although MCL may rarely show plasmacytic differentiation, ancillary studies are needed to exclude a composite lymphoma.

1736 Distinct Expression Pattern of TRAIL in Normal and Colon Carcinoma Cells: A Novel Chemopreventive/Therapeutic Target

KA Matkowskyj, J Liao, YT Chung, G-Y Yang. Northwestern University, Chicago, IL.
Background: TRAIL is a cytotoxic protein that induces apoptosis via its death receptors. TRAIL acts following binding to one of the 4 receptor subtypes. TRAIL-R1/DR4 and TRAIL-R2/DR5 contain an intracellular death domain, while TRAIL-R3/TRID and TRAIL-R4 are decoy receptors preventing apoptosis. PPAR-γ is a nuclear receptor found in epithelial neoplasms such as colon. PPAR-γ is activated by prostaglandin J_2 (PGJ_2) and has been shown to induce suppression and reversal of malignant changes in colon cancer in vitro by regulation of NF-κB, c-myc, and β–catenin. Regulation of c-myc results in upregulation of DR5 and blockade of c-FLIP. Thus, the main objectives

of this study were to determine TRAIL receptor expression in normal and a malignant colon cancer cell line and to determine the role of combination therapy using PGJ_2 and TRAIL on colonic cell apoptosis.
Design: Expression of the 4 TRAIL receptors in the human normal colonic epithelial cell line NCM460 and colonic carcinoma cell line HT-29 were examined using a real-time PCR approach with GAPDH as a reference gene. Dose effect of TRAIL on apoptosis induction was determined by morphologic criteria and trypan blue stain. Synergistic effects of PGJ_2 and TRAIL was examined by co-treatment using 3 dose combinations. All experiments were repeated (n=5) to assure statistical significance and power. Further quantitative determination of TRAIL-related pathways was also performed using western blot.
Results: Quantitative RT-PCR revealed a distinct expression pattern of TRAIL-R in normal and carcinoma cell lines; it showed an increase in death receptor and decrease in decoy receptor expression in carcinoma cells compared to normal colonic epithelial cells; DR4 was 5.5-fold and DR5 expression was 17.2-fold higher than in normal cells. In contrast, the expression of the decoy receptors TRID and TRAIL-R4 was significant lower than normal cells (0.03 and 0.622-fold, respectively). Treatment of HT-29 cells with TRAIL for 48 hours revealed ~30% induction of apoptosis. A significant increase in apoptosis was seen in HT-29 cells co-treated with PGJ_2 and TRAIL (60% induction). Further downstream regulation of the TRAIL pathway by PGJ_2 was also studied.
Conclusions: A distinct expression profile of death/decoy TRAIL receptors is present between the normal and carcinoma colonic cell lines, suggesting TRAIL death receptors would be a unique therapeutic target for treatment of colonic cancer with the combination of PGJ_2 and TRAIL as a novel approach to induce cancer cell death.

1737 Identification of Ubiquitin E3 Ligase c-Cbl as a Novel Angiogenesis-Suppressor Protein

M Mehta, D Husain, E Ahmed, W Pfeifer, N Rahimi. Boston University, Boston, MA; Boston University, Boston.
Background: A crucial aspect of many human diseases such as cancer, inflammatory diseases, and age-related macular degeneration is the formation of new blood vessels known as angiogenesis. In angiogenesis, VEGF activation of VEGF receptor-2 (VEGFR-2) leads to tyrosine phosphorylation of Phospholipase C- gamma 1(PLC-g1). Abolishing PLC-g1 binding site on VEGFR-2 has shown to inhibit endothelial cell tube formation, proliferation and angiogenesis. Previous work from our laboratory demonstrates that Casitas B-lineage lymphoma (c-Cbl) promotes ubiquitination of PLCg1 and suppression of its tyrosine phosphorylation (Singh *et al*., PNAS 2007). This study is designed to evaluate the role of c-Cbl in pathological angiogenesis in null c-Cbl mice.
Design: Endothelial cells were isolated from wild type and c-Cbl null mice and assayed for their ability to proliferate in response to Vascular Endothelial Growth Factor (VEGF). Western blot analysis was used to analyze PLCg1 activation in wild type endothelial cells versus c-Cbl null cells. In vivo angiogenesis assays including laser-induced choroidal neovascularization (CNV) and tumor-induced angiogenesis were performed. CNV was induced by laser photocoagulation (50µ, 0.1 seconds, 200 mw). 14 lesions were induced in the eyes of nude mice and 18 lesions in those of control mice. These lesions were documented at days 7, 10, 14 and 21 with fundus photography and angiography for progression, size and leakage from the CNV. The mice were sacrificed at week 4 and the enucleated eyes were frozen, sectioned and histologically evaluated. Hematoxylin and eosin (H&E) staining and immunoperoxidase staining with CD31 and phospho-PLCg1 antibodies were performed.
Results: Laser-induced choroidal neovascularization (CNV) lesions in the c-Cbl knockout mice were significantly more in number, more confluent and increased in size with time compared to control wild type mice. The enhanced angiogenesis was also observed in VEGF- and tumor-induced angiogenesis in c-Cbl null mice. Immunoperoxidase staining with CD31 (antibodies demonstrating endothelial cells) and phospho-PLCg1 antibodies in the c-Cbl knockout mice confirmed the enhanced activation PLCg1 in endothelial cells.
Conclusions: The data showed that loss of c-Cbl results in increased activation of PLCg1 and enhanced proliferation of endothelial cells *in vitro*. Altogether, our in vitro and in vivo analysis for the first time identifies c-Cbl as a novel angiogenesis-suppressor protein.

1738 General Morphological Features, Ki-67 and Telomerase/Telomere Reliably Predict Common Malignancies and Subclassify Carcinomas

J Moorhead, J Gonzalez, A Blanes, SJ Diaz-Cano. King's College Hospital, London, United Kingdom; University of Malaga School of Medicine, Malaga, Spain.
Background: Tumor subclassification relies heavily on immunohistochemical markers and is site specific. Biological definition based on general morphology and kinetic regardless of location is not available.
Design: We analyzed primary and secondary growth patterns (tubulo-papillary, nested-trabecular, nodular-solid, diffuse), nuclear grade (including chromatin, nucleolus, pleomorphism and anisokaryosis), desmoplasia, and confluent necrosis in common malignancies: carcinomas (45 basal cell, 75 squamous cell, 104 adenocarcinomas, 30 urothelial, and 15 neuroendocrine), sarcomas (75), lymphomas (75) and melanomas (45). Representative samples were evaluated by standard immunohistochemistry for Ki67, telomerase, mlh1, msh2, TUNEL assay for apoptosis, telomere PNA-FISH, and selective cDNA miniarray (telomerase, p53, mdm2, p21, cdk2, cyclin E, pRB, Egr2, JunB, and FosB). Total RNA was extracted, cleaned from normal and neoplastic tissues (RNeasy columns), first-strand cDNA synthesized using T7-(dT24)-oligomer and used as template for cRNA synthesis. The cRNA was fragmented, Cy3-/Cy5-labeled, and hybridized to miniarray noncompetitively, cross-validating the results (expression factor>2, significance<0.01). Appropriate controls were run. Fisher's exact tests and analysis of variance (significant if $P<0.05$) were used for comparison; significant variables were used for cross-validated discriminant analyses for a biological definition by diagnostic groups.
Results: Discriminant analysis for the main diagnostic groups selected as independent variables growth patterns, nuclear pseudoinclusions, necrosis distribution, Ki-67 index, desmoplastic reaction and nuclear grade (nucleolus number, chromatin distribution and pleomorphism). Telomerase expression and telomere positive cells (%) were the added variables for carcinoma subclassification. The percentage of cases correctly classified with these variables were always >97% in all cross-validated models. Telomerase/telomere indices directly correlated with the kinetic index, being significantly higher in high-grade malignancies with upregulation of p53, cyclin E, Egr2, JunB and FosB.
Conclusions: A careful selection of a small number of morphological (growth patterns, desmoplastic reaction, nuclear grading) and kinetic features provides a reliable and reproducible classification of common malignancies. Proliferation and telomerase/telomere indices improve the prediction for carcinoma subclassification only.

1739 Detection of *FOXO1A*, *SYT* and *DDIT3* Gene Break Aparts by Fluorescence In-Situ Hybridization in Various Carcinomas of Epithelial Origin

S Narendra, J Tull, S Zhang. SUNY Upstate Medical University, Syracuse, NY.
Background: *FOXO1A, SYT* and *DDIT3* gene break-aparts associated with chromosomal translocations can be identified in the majority of alveolar rhabdomyosarcomas, synovial sarcomas and myxoid liposarcomas, respectively, and have been widely used as specific molecular markers in diagnosis of these neoplasms. However, the frequency and specificity of these genetic markers as well as their clinical utility in carcinomas of epithelial origin have not been studied.
Design: Tissue samples ranged from small biopsies to wide resections, diagnosed from 2000 to 2007. Commercial probes of fluorescence in situ hybridization (FISH) for *FOXO1A*, *SYT* and *DDIT3* gene break aparts were applied in 43, 42 and 31 cases respectively of paraffin embedded tissues of different carcinomas. The carcinomas included the tissue origins of breast, ovary, lung, thyroid, urinary bladder, cervix, pancreas, parotid, adrenal, gallbladder, kidney, skin, colon, testes and larynx.
Results: With appropriate positive and internal controls, there were no *FOXO1A*, *SYT* or *DDIT3* gene breaks identified in 43, 42 and 31 cases of carcinomas, respectively.
Conclusions: *FOXO1A*, *SYT* and *DDIT3* gene break aparts are extremely rare events, if any, in various carcinomas of epithelial origin, and remain specific biomakers for alveolar rhabdomyosarcoma, synovial sarcoma and myxoid liposarcoma respectively.

1740 Rosiglitazone Impairs Proliferation of Human Adrenocortical Cancer: Preclinical Study in a Xenograft Mouse Model

G Nesi, M Mangoni, M Pepi, S Gelmini, T Ercolino, C Orlando, M Mannelli, M Luconi. University of Florence, Florence, Italy.
Background: Adrenocortical carcinoma (ACC) is a rare aggressive tumor with a poor prognosis. The lack of a specific and effective medical treatment is due to the poor knowledge of the mechanisms underlying tumor growth. Research on potential drugs able to specifically inhibit tumor proliferation is essential in order to develop more efficacious therapies.
Design: We evaluated the *in vivo* effect of rosiglitazone (RGZ), an anti-diabetic drug with *in vitro* anti-tumor properties, on ACC proliferation in a xenograft model obtained by subcutaneous injection of human ACC H295R cells in athymic mice. When the tumor size reached 5 mm, the animals were allocated to 5mg/kg RGZ- or water-treated groups. Tumor volume was measured twice a week.
Results: A significant reduction of tumor growth in the RGZ versus the control group was observed and was already maximal following 17 days of treatment [1-T/C=75.4% (43.7-93.8%)]. After 31 days, the mice were sacrificed and the tumors analyzed. Histologically, in the control group, the tumors displayed a solid, diffuse architecture and consisted of rather small, uniform cells with coarse chromatin and prominent nucleoli. A mixture of large caliber vessels and a disorganized network of small-caliber vessels were evident. A remarkable number of mitotic figures was present, often with atypical forms. Conversely, in the RGZ group, the tumors showed well-demarcated borders, a lower degree of vascularization, a greater number of apoptotic bodies and a lower mitotic index. Immunohistochemistry demonstrated that Ki-67 was reduced in the RGZ *versus* the control group. Quantitative-real-time RT-PCR showed a significant reduction in the expression of angiogenic (VEGF), vascular (CD31), proliferation (BMI-1) and anti-apoptotic (Bcl-2) genes in RGZ *versus* control group tumors. The same inhibitory effects were confirmed in *in vitro* RGZ-treated H295R.
Conclusions: Our findings support and expand the role of RGZ in controlling ACC proliferation and angiogenesis *in vivo* and *in vitro*.

1741 Extra-Lysosomal Localization of Arylsulfatase B: Implications for Epithelial Pathobiology

SV Prabhu, G Guzman, S Bhattacharyya, AK Balla, JK Tobacman. University of Illinois at Chicago, Chicago, IL; Jesse Brown VA Medical Center, Chicago, IL.
Background: Arylsulfatase B (ASB; N-acetylgalactosamine-4-sulfatase) is deficient in MPS VI, the lysosomal storage disease characterized by accumulation of chondroitin-4-sulfate and dermatan sulfate. Recent work demonstrated reduction of ASB activity in patients with cystic fibrosis and in malignant mammary epithelial cell lines. In colonic epithelial cell lines, reduced ASB activity was associated with increases in cell migration, RhoA activation and MMP9 expression. Surprisingly, immunohistochemistry (IHC) and activity assays demonstrated ASB in cell membranes of cultured human bronchial and colonic epithelial cells, as well in the cytoplasm and nuclei.
Design: To further assess localization of ASB in normal and malignant colonic epithelial cells, we measured ASB activity using the substrate 4-MUS in a quantitative fluorometric assay. IHC of ASB was assessed in 75 cores in tissue microarrays from the National Disease Research Interchange (Philadelphia, PA). A rabbit polyclonal antibody (Open

Biosystems, Huntsville, AL) directed at a unique C-terminal epitope and shown to be specific for ASB was used for IHC. Three observers independentlly reviewed each of the sections, assessing % positivity and intensity of cytoplasmic, nuclear, and luminal membrane staining.
Results: In normal colonic tissue, IHC demonstrated marked prominence of ASB in the luminal membrane. In malignant tissue, luminal membrane staining was reduced or absent. Increased cytoplasmic intensity was apparent near the luminal surface in the normal tissue, in contrast to deeper in the crypts. This variation was absent in the malignant cells. In the normal tissue, rare, isolated cells, with intense, uniform cytoplasmic and nuclear staining, were dispersed in the crypts. Nuclear staining was generally absent in the malignant epithelial cells; when present, staining was punctate. Activity assay demonstrated that ASB activity was significantly less in malignant colonic tissue than in normal tissue (56.3 ± 4.0 vs. 108.1 ± 7.8 nmol/mg protein/hr; $p<0.0001$, unpaired t-test, two-tailed, n=6).
Conclusions: The enzyme ASB is not confined to lysosomes in colonic epithelial cells, but also has luminal membrane localization. The distinct cellular pattern of ASB staining in the normal colonic epithelial cells is lost in the malignant tissue, and ASB activity is significantly reduced. ASB may be a useful marker of colonic pathology.

1742 p53-Mediated Apoptosis in Multiple Myeloma Cells: Evidence for a Transcription-Independent Pathway

MN Saha, A Asuma-Mukai, H Chang. University Health Network, University of Toronto, Toronto, Canada.
Background: The p53 protein plays a key role in the apoptotic response of various hematological malignancies. Although p53-mediated apoptosis is conventionally followed by transcriptional regulation of p53-target genes, non-transcriptional mitochondrial p53 mediated apoptotic pathway has been identified in cancer cells. As the functional consequence p53 signaling in multiple myeloma (MM) is not clearly understood, here we explore the molecular mechanisms of apoptosis in myeloma cells mediated through activation of the p53 pathway by an MDM2 antagonist, nutlin.
Design: Human MM cell lines (MM1.S and H929 cell lines harboring wild type p53; and LP1 and U266 cell lines harboring mutant p53) and primary MM samples were exposed to nutlin, and assessed for cell viability, cell cycle analysis and apoptosis.
Results: Treatment of MM cells with nutlin resulted in a reduction in cell viability, an increase in the apoptotic fraction, and cell cycle arrest in MM1.S and H929 as well as 3 of the 5 primary MM samples tested. These effects were accompanied by up-regulation of p53 and induction of p53-dependent proteins p21, MDM2, puma, bax and Bak; and down-regulation of anti-apoptotic proteins, Bcl2 and survivin. By contrast, no effects on cell cycle arrest or apoptosis were found in MM cell lines harboring mutant p53. Aside from nuclear stabilization, nutlin caused cytoplasmic p53 accumulation and translocation to mitochondria, associated with cytochrome C release that precedes the induction of p53 target genes. Importantly, although pifithrin-α (PFT-α), an inhibitor of p53-mediated transcription, inhibited the nutlin-induced up-regulation of p53-transcriptional targets, surprisingly augmented apoptosis by ~ 2 fold. Furthermore, immunoprecipitation with an anti-Bcl2 antibody showed co-precipitation of Bcl2 and p53 from lysates (mitochondrial fractions) of MM1.S cells treated with nutlin.
Conclusions: Our data suggest that a transcription-independent pathway involving direct binding of p53 to mitochondrial anti-apoptotic proteins plays a major role in p53-mediated apoptosis in MM cells; the transcriptional targets of p53 may include proteins that inhibit non-transcriptional pathway. Thus, therapeutic strategies aimed at inhibiting up-regulation of p53-mediated transcription together with administrating non-genotoxic drugs such as nutlin may hold promise for the treatment of MM patients who are relatively drug resistant.

1743 Holoclone and Non-Holoclone Derived Cell Lineage Characterisation Analysis in Prostate Cancer

YM Salley, MF Gallagher, PC Smyth, CM Martin, OM Sheils, JJ O'Leary. Trinity College, Dublin 2, Ireland.
Background: Prostate cancer is a heterogeneous disease and is the second most common cause of cancer resulting in male deaths. Stem-like cells have been identified in several malignancies including prostate cancer and are thought to drive primary tumorigenesis through self-renewal and differentiation. Additionally, persistence of stem cells post therapeutic intervention has been proposed as an explanation for metastasis and recurrence. Holoclones are a tightly packed clone of small cells generally thought to contain stem cells and progenitors. The aim of this study was to derive holoclones from prostate cancer cell lines and to characterise their expression.
Design: In this study, holoclones were cultured using a high salt-soft agar assay for LNCaP (metastatic carcinoma) and PC-3 (non-metastatic adenocarcinoma) cell lines. The expression of a panel of key stemness genes and pathways, was assessed in a group of prostate holoclones derived from cell lines LNCaP and PC-3 using a quantitative Real Time TaqMan® PCR method.
Results: Holoclones were generated from cell lines (LNCaP, PC-3) using a high salt-soft agar assay. LNCaP holoclones were maintained for 24 days and PC-3 holoclones were maintained for 6 days. The differential duration of the time points denotes that the LNCaP cell line represents a metastatic prostatic carcinoma and should contain a higher number of cancer stem cells. In combination, stemness genes were used to exemplify the stem cell potential and characteristics of these hololcones. Examples of stemness genes include Sonic Hedgehog, TGF-β, Oct4 and Nanog.
Conclusions: Expression profiles were generated for genes representing stemness. LNCaP and PC-3 holoclones both indicated stemness characteristics. However both LNCaP and PC-3 holoclones expressed different stemness markers and this disparity was also further represented by the duration differences in time points. Future work will consist of further characterisation and analysis of LNCaP and PC-3 holoclones.
Acknowledgements: Prostate Cancer Research Consortium

1744 Histopathological Features of Mouse Models of Embryonal Rhabdomyosarcoma

DP Schuetze, K Nishijo, LD Hampton, AT McCleish, C Keller, BP Rubin. Cleveland Clinic, Cleveland, OH; University of Texas Health Science Center, San Antonio, TX.
Background: Embryonal rhabdomyosarcoma (ERMS) is a rare tumor that occurs predominantly in children. We have developed a set of conditional mouse models of ERMS to understand the cell of origin and provide a preclinical platform for testing new therapies.
Design: Conditional mouse models of ERMS were developed using Cre:loxP and targeted knock-in technology. This model utilizes satellite cell, myoblast or myofiber-specific expression of Cre recombinase to delete combinations of *Ptch*, *p53*, and/or *Rb,* tumor supressors associated with human ERMS. Seventy-six lesions were examined with hematoxylin and eosin and also trichrome. Immunohistochemical studies for desmin and myogenin (and MyoD1 for several cases) were performed. The general histologic features were described and rhabdomyoblasts, cross striations, and reactivity for desmin, myogenin, and MyoD1 were noted. A histologic classification was rendered for each case.
Results: Seventy six tumors were classified. Thirty-one (41%) were classified as ERMS. Features common to these cases included fascicles of spindle cells with eosinophilic cytoplasm, cytoplasmic reactivity with desmin (29/29 tested cases, 100%), and nuclear reactivity with myogenin (22/27 tested cases, 81.5%) and/or MyoD1 (4/5 tested cases, 80%). A majority of cases (18/31; 58%) contained rhabdomyoblasts. Cross striations occurred in 13/31 (42%). Other subtypes of rhabdomyosarcoma (RMS) were seen, including 4 cases of alveolar RMS and 2 cases of pleomorphic RMS. Eleven tumors were classified as spindle cell sarcoma with possible myogenic differentiation, as histologic and/or immunophenotypic criteria of unequivocal ERMS were not met. Other malignancies occurred, including 4 cases of osteosarcoma, 9 cases of spindle cell sarcoma, not otherwise specified, 1 case of malignant epithelioid neoplasm, not otherwise specified, and 3 cases of lymphoma.
Conclusions: These conditional mouse models of ERMS generate tumors with histologic and immunophenotypic characteristics similar to those seen in human ERMS in approximately 41% of the lesions. Since not all lesions that develop are ERMS, histopathological examination will play a crucial role in studies involving these models. The continuity between spindle cell sarcomas and ERMS for some models suggests that certain myogenic cells of origin can give rise to a spectrum of poorly vs well differentiated tumors.

1745 Constitutive Overactivation of Phospholipase D/mTORC2 Pathway in Uterine Leiomyosarcomas vs STUMPs, Leiomyomas and Myometria

Q Shen, X Duan, ME Rodriguez, S Dhingra, RE Brown. The University of Texas Medical School at Houston, Houston, TX.
Background: mTOR exists in two complexes: mTORC1 and mTORC2. mTORC1 is predominantly cytoplasmic and sensitive to rapamycin, while a significant proportion of mTORC2 is nuclear and relatively resistant to rapamycin. We previously reported mTOR was constitutively activated in uterine leiomyosarcomas; this activation specifically occurred in the nucleus, suggesting a role for mTORC2, not mTORC1, in leiomyosarcoma tumorigenesis. Unlike mTORC1, which is known to be activated by PI3K/Akt, little is known about the regulation of mTORC2 activity. Recently phospholipase D (PLD) and its metabolite phosphatidic acid (PA) have emerged as an alternative regulator of the mTOR signaling-binding of PA activates both mTORC1 and mTORC2; the effect of PA is competitive with rapamycin. In this study, we investigated the expression of the two major PLD isoforms, PLD1 and PLD2, and one of the key downstream mediators of mTORC2, p-Akt (Ser473) in the leiomyosarcomas (LMS), uterine smooth muscle tumors of uncertain malignant potential (STUMPs), leiomyomas (LM) and normal myometria.
Design: A formalin-fixed, paraffin-embedded tissue microarray was constructed including 12 LMS, 8 STUMPs, 17 LM, and 11 normal myometria. Immunohistochemistry was used to detect PLD1, PLD2, and p-Akt (Ser473). Protein expression was quantified with brightfield microscopy regarding staining pattern, cellular percentage and intensity.
Results: PLD2 expression is predominantly in the nucleus. Strong PLD2 expression is seen in 83% LMS, 38% STUMPs versus 12% LM and 9% in controls. As for PLD1, nuclear expression is the main pattern in LMS, whereas faint cytoplasmic staining is the main pattern in all other groups. Moderate PLD1 expression is seen in 59% LMS but none in STUMPs, LM or controls. mTORC2 phosphorylates Akt at Ser473. In line with our prior findings on p-mTOR, p-Akt (Ser473) also resides largely in the nucleus in LMS. In contrast, it exhibits weak cytoplasmic and nuclear expression in all other groups. Strong p-Akt staining is seen in 59% LMS versus 12% STUMPs, and 0% in LM and controls.
Conclusions: We report for the first time that PLD is overexpressed in uterine leiomyosarcomas. Our data show the PLD/mTORC2 pathway is constitutively overactivated in leiomyosarcomas, evidenced by nuclear co-localization and overexpression of PLD1, PLD2, p-mTOR and p-Akt (Ser473). These findings provide a rationale for targeting PLD activity to enhance the efficacy of rapamycin in leiomyosarcomas.

1746 Constitutive Overactivation of Phospholipase D1/mTORC2 Pathway in Endometrial Carcinomas

Q Shen, RE Brown, ML Stanton, X Duan. University of Texas Medical School at Houston, Houston, TX.
Background: mTOR assembles into two complexes. mTORC1 is predominantly cytoplasmic and sensitive to rapamycin, whereas mTORC2 is abundant in both cytoplasm and nucleus, and relatively resistant to rapamycin. Previously we reported mTOR overactivation was consistently seen in endometrial carcinoma (ECa); this activation predominantly occurred in the nucleus, indicating an essential role for mTORC2, not mTORC1 signaling in endometrial tumorigenesis. In line with this, in

clinical trials rapamycin shows efficacy against only a limited number of ECa. Recently phospholipase D (PLD) and its metabolite phosphatidic acid (PA) have been shown to regulate the mTOR signaling-binding of PA activates both mTORC1 and mTORC2; the effect of PA is competitive with rapamycin, with much higher concentrations of rapamycin needed to inhibit the PA-mTORC2 interaction than PA-mTORC1. In this study, we evaluated the expression of the two major PLD isoforms, PLD1 and PLD2, and one of the downstream effectors of mTORC2, p-Akt (Ser473) in ECa, proliferative (PE) and secretory endometrium (SE).
Design: A formalin-fixed paraffin-embedded tissue microarray containing 33 ECa, 24 PE, and 21 SE was constructed. IHC was used to detect PLD1, PLD2, and p-Akt (Ser473). Protein expression was quantified with light microscopy regarding staining pattern, cellular percentage and intensity.
Results: PLD1 expression is seen in both cytoplasm and nucleus. Moderate PLD1 expression is noted in 37% ECa but none in PE or SE; moreover, 71% PE and 71% SE show a complete lack of PLD1 expression. PLD2 expression is largely in the nucleus. No differences in the level of PLD2 expression are seen among the three groups. It is known mTORC1 phosphorylates p70S6K at Thr389, while mTORC2 phosphorylates Akt at Ser473. In line with our prior data showing predominant mTORC2 activation in ECa, expression of p-Akt (Ser473) is markedly increased in ECa compared to its non-cancerous counterparts: moderate to strong cytoplasmic and nuclear p-Akt (Ser473) staining is seen in 64% ECa vs 21% PE, and 5% SE. In contrast, there is no significant difference in expression of p-p70S6K (Thr389) among ECa, PE, or SE (prior data).
Conclusions: To our knowledge this is the first report of overexpression of PLD in ECa. Our data show the PLD1/mTORC2 pathway is constitutively overactivated in ECa, and suggest that suppressing PLD activity may represent a means for improving the efficacy of rapamycin in ECa, where the rapamycin-insensitive mTORC2 is the dominant driving force of tumorigenesis.

1747 A Novel Locus for Autosomal Dominant Restless Legs Syndrome

EB Skehan, MMA Abdulrahim, CK Hand, NA Parfrey. University College Cork, Cork, Ireland.
Background: Restless Legs Syndrome (RLS) is a sleep-related disorder characterised by an irresistible urge to move the lower limbs associated with unpleasant sensations. Symptoms present while at rest, generally in the evening, and are relieved, at least partially and temporarily, by movement. RLS affects 5-10% of the general population, frequently resulting in chronic sleep deprivation. Drugs targeting the dopamine pathway have shown therapeutic benefit. RLS may develop secondary to conditions such as renal failure, iron deficiency and pregnancy. More commonly, RLS is a familial disorder inherited in an autosomal dominant manner. RLS loci have been identified in six distinct genomic regions by linkage analysis. Association mapping has highlighted a further four areas of interest. To date, no causative gene has been identified.
Design: We recruited a three generation Irish family with autosomal dominant RLS. Eighteen members participated in this study of whom 11 are affected. Institutional ethical approval was obtained and all participants gave written informed consent. Symptom questionnaires were completed and neurological examinations were undertaken. Genomic DNA was extracted from venous blood samples. Polymorphic microsatellite markers were amplified by PCR and samples were genotyped using the ABI3130 genetic analyser. LOD scores were generated using FASTLINK software.
Results: Linkage was excluded from all known RLS loci. A genome-wide scan identified a region of linkage with a maximum LOD score of 3.59, at a theta value of 0. Recombination events, identified by haplotype analysis, define a genetic region which corresponds to 2.5 Mb. This disease gene containing region has approximately 100 known genes. A number of candidate genes have been identified based on potential involvement in RLS pathogenesis and are the subject of further study.
Conclusions: We have successfully identified a novel locus for autosomal dominant Restless Legs Syndrome. Completion of this stage of the study enables us to attempt to identify the causative gene in this family and, thus, to further the understanding of RLS pathogenesis.

1748 Cyclin B1 Correlates with the Grade of Cervical Dysplasia

WU Todd, JF Silverman. Allegheny General Hospital, Pittsburgh, PA.
Background: Cyclin B1 is a key molecule involved in the transition from G2 to M phase of the cell cycle and interacts with both pRB and p53. Cyclin B1 expression has been shown to correlate with pRB expression in certain tumors, but its expression in cervical dysplasia has not been previously reported.
Design: 72 cases of normal cervix and cervical dysplasia were retrieved for immunohistochemical analysis. The cases encompassed 8 normal, 24 cervical intraepithelial neoplasia (CIN) I, 21 CIN II and 22 CIN III. Immunohistochemical analysis was performed using antibodies directed against p16 and cyclin B1. Positive staining was quantitatively and qualitatively recorded. The fisher exact test and paired T-test were used to determine significance.
Results: Cyclin B1 positive cells localized to the basal 2-3 cell layers in normal cervical biopsies in low numbers. In contrast, dysplastic cervical epithelium showed both an increase in the number of cyclin B1 positive cells and localization to both the basal and superficial layers of the epithelium ($P<0.01$). The number of cyclin B1 positive cells increased with the grade of cervical dysplasia. There was clear separation of normal biopsies from cervical dysplasia and the grades of dysplasia based on the number of cyclin-B1 positive cells without overlap of the 95% confidence intervals.
Conclusions: There are both quantitative and qualitative differences between the staining patterns of normal and various grades of dysplastic cervical epithelium with cyclin B1, a previously unreported finding. The number of cyclin B1 positive cells correlates well with the progressive grade of cervical dysplasia. Cyclin B1 may therefore have a role in the pathobiology and progression of cervical dysplasia and serve as an aid in grading low from high grade dysplasia.

1749 Microscopic 3-Dimensional Reconstruction of Prostate Cancer Cell Network: An Innovative Approach To Perceive Tumor Invasion

AV Ugolkov, LJ Eisengart, Y Jiang, Y Peng, XJ Yang. Northwestern University, Chicago, IL; University of Chicago, Chicago, IL.
Background: Conventional cancer research is based on microscopic observation of 2D (2-dimensional) section of tumor tissue. Matrigel in vitro experiments and 2D tumor sections give an impression that cancer cells can migrate withing normal tissue supporting epithelial-mesenchymal transition (EMT) theory. The aim of this study was to reconstruct microscopic 3D (3-dimensional) figure of prostate cancer cell network to address the question whether cancer cells can invade as migrating independent cells or small clumps of cells as seen on 2D tumor section.
Design: To facilitate a subsequent detection of cancer cells using computer image-analysis techniques, E-cadherin immunostaining was performed using 100 serial prostate cancer sections. We developed and used a software which allows to recognize malignant cells (brown) vs. stromal cells (blue). In order to expand conventional 100 serial 2D images into one 3D figure of prostate tumor, we used computer image-analysis techniques.
Results: We selected the area of tumor invasion front representing mostly prostate cancer cells surrounded by stromal cells. After scanning of 100 serial 2D tumor sections stained for E-cadherin and subsequent recognition of E-cadherin positive cancer cells by software, we used computer image-analysis techniques to delete benign epithelial and stromal cells from images and reconstruct prostate cancer cell network in 3D. We found that cancer cells are not separated (as seen on 2D section) but connected forming cancer cell network in 3D figure resembling "hair ball" where free of cancer cell space is filled with benign cells. Our results suggest that tumor invasion is driven by not migration but proliferation of cancer cells leading to elongation of tumor invasion roots and formation of new buds or branches from existing roots.
Conclusions: 3D histology is an innovative concept that challenges conventional concepts of cancer invasion based on analysis of 2D tumor sections. Our analysis of 3D configuration of prostate cancer cell network suggests proliferation of cancer cells leading to formation of tumor invasion roots as a critical determinant of microscopic tumor invasion. By careful reconstruction and investigation of 3D microscopic figure of tumor, we can achieve a better understanding of tumor invasion which could be a basis for the development of new approaches in cancer prevention and therapy.

1750 Sophorolipids Decrease Pulmonary Inflammation in a Mouse Asthma Model

H Vakil, S Sethi, S Fu, A Stanek, S Wallner, R Gross, MH Bluth. Wayne State School of Meidcine, Detroit, MI; SUNY Downstate Medical Center, Brooklyn, NY; Polytechnic University, Brooklyn, NY.
Background: Sophorolipids are promising modulators of the immune response. We have previously demonstrated that sophorolipids decreased (1) sepsis related mortality in preclinical models, (2) IgE production through downregulation of IgE regulatory genes *in vitro* and (3) OVA specific IgE in BAL fluid *in vivo*. Here we investigated the effects of sophorolipids on pulmonary inflammation and molecular profiles in an *in vivo* asthma model.
Design: Black c-57 mice were challenged with ovalbumin (OVA) via IP injection/nebulization. Sophorolipids or sucrose vehicle control was administered via nebulization pre and post full OVA asthmatic insult and animals were sacrificed after 14 days. Lung tissue was obtained and assessed for asthma severity determined by (1) perivascular and peribronchial inflammation (histopathology) and (2) expression of Galectin 3, NFκB and Mucin1/2 (immunohistochemistry). Data are reported as mean observations of 10 scanned fields/mouse (100x magnification) and significance between groups was determined by student's t-test.
Results: Lungs obtained from mice exposed to full OVA induction regimen demonstrated pulmonary evidence of asthma as evidenced by perivascular and peribronchial inflammation which was decreased with nebulized sophorolipids (perivascular: 13 vs 6, $p=0.05$; peribronchial 12 vs 5, $p=0.004$). Furthermore, sophorolipid treated animals had a 50% increase in perivascular expression of Galectin3 compared with vehicle-treated asthmatic mice (4 vs 8, $P=0.03$). However expression of NFκB, MUC 1 and MUC2 did not differ between treated and control animals. No adverse effects were observed at all doses tested.
Conclusions: Sophorolipids decreased asthma severity in experimental asthma (>50%) by modulation of pulmonary inflammation and Galectin 3. These data continue to support the utility of sophorolipids as an anti-inflammatory agent and novel potential therapy in allergic asthma.

1751 Differential Expression of Spectrin Isoforms in Benign and Malignant Epithelial Tumors

Y Wang, J Albanese, H Ratech. Albert Einstein College of Medicine/Montefiore Medical Center, Bronx, NY.
Background: Spectrin is a rod-like, multifunctional molecule composed of an α-subunit and a β-subunit. There are multiple spectrin isoforms that can bind actin and associate with other proteins to help integrate structure and function in complex tissues. Because embryonic liver fodrin, a variant of β-spectrin, has recently been implicated in the pathogenesis of hepatocellular carcinoma, we hypothesized that various spectrin isoforms might be involved in other epithelial tumors. We report the first comprehensive study of the expression and localization of spectrin isoforms in normal human epithelial tissues and in their benign and malignant counterparts.
Design: We retrospectively studied the expression of spectrin isoforms αI, αII, βI, βII and βIII by immunohistochemical staining of normal epithelial tissues as well as benign and malignant neoplasms from 66 specimens involving breast, colon, kidney, liver, prostate, thyroid, uterine cervix and transitional epithelium of urinary bladder.
Results: The majority of normal epithelial cell types expressed αII spectrin. Normal uterine cervical squamous mucosa expressed αII spectrin in the basal and parabasal cells,

but not in the keratinized superficial layers; the pattern for βI spectrin was the inverse for αII spectrin. For example, we found βI spectrin in the superficial, but not in the basal epithelium of the uterine cervix. Compared to their normal epithelial counterparts, there was loss of αII spectrin in papillary thyroid carcinoma, in clear cell renal carcinoma and in invasive ductal breast carcinoma. Expression of βI spectrin was limited to normal hepatocytes, transitional umbrella cells of the bladder, type II pneumocytes of the lung, mature superficial squamous epithelium of the uterine cervix, and lobular and ductal epithelium of the breast. In contrast to the absence of staining for βI spectrin in normal biliary ductules, thyroid follicles and renal tubules, we detected aberrant expression of βI spectrin in biliary ductal carcinoma, thyroid papillary carcinoma and renal clear cell carcinoma. Spectrin isoforms βII and βIII were universally present in both benign and malignant epithelial tumors.
Conclusions: Loss or gain of specific spectrin isoforms occur both during normal epithelial maturation and in some examples of neoplastic transformation. This suggests the possibility of a significant role for spectrin isoforms in carcinogenesis.

1752 MDM2 Amplification in Atypical Lipomatous Tumors/Well-Differentiated Liposarcomas and Dedifferentiated Liposarcomas: A Comparative RT-PCR and FISH Study

JG Willems, M Gjihaderi, A Olsson, M Lestrin, G Elmberger. Karolinska University Hospital Solna, Stockholm, Sweden.
Background: As future therapeutic options for well-differentiated and dedifferentiated liposarcomas are likely to include targeting the MDM2 pathway, reliable methods for its demonstration will be required. A comparative study of the sensitivity of RT-PCR versus FISH for demonstrating amplification of MDM2 in such tumors was therefore performed.
Design: 30 consecutive resected atypical lipomatous tumors/well-differentiated liposarcomas and dedifferentiated liposarcomas as well as 6 control adipocytic tumors of different type, were reviewed by two pathologists and subsequently investigated for amplification of MDM2. Genomic DNA was extracted from formalin fixed paraffin embedded tissues using the Qiagen Qia Amp FFPE kit. Fifty nanogram of each FFPE DNA was used in a multiplex real-time PCR reaction using the FAM (MDM2) and VIC (RNase P as internal control) labeled probes on an ABI prism 7000. To distinguish samples with high MDM2 copy number from those with normal copy number, the standard delta-Ct method was used. Neoplasms with high copy number were judged to be amplified. FISH dual copy assay was performed using Poseidon Repeat Free MDM2 (12q15) & SE12 control probe. More than 4 signals were considered evidence of amplification.
Results: 1-On FISH analysis 29 of 30 atypical lipomatous tumors/well-differentiated liposarcomas and dedifferentiated liposarcomas were found to be amplified for MDM2, whereas 1 case of dedifferentiated liposarcoma was not. 2- On RT-PCR analysis of the same 30 tumors, 28 showed MDM2 amplification. Unamplified were the above mentioned case of dedifferentiated liposarcoma and 1 case of well-differentiated liposarcoma of inflammatory type. 3- None of the adipocytic tumors of other type showed MDM2 amplification by either mehod.
Conclusions: In atypical lipomatous tumors/well-differentiated liposarcomas and dedifferentiated liposarcomas demonstration of MDM2 amplification as measured by FISH was 96,6 % and by RT-PCR 93,3 %. Following methodological adjustments results could be improved.

1753 15-Lipoxygenase 1 Promotes Hypoxia-Inducible Factor 1α Degradation Dependent of Essential Enzymatic Function

H Zhong, R Wang, U Kelavkar, M Ohh, JW Simons. New York University School of Medicine, New York; Emory University School of Medicine, Atlanta; University of Pittsburgh School of Medicine, Pittsburgh; University of Toronto, Toronto, Canada.
Background: Hypoxia inducible factor-1α (HIF-1α) is the major subunit of HIF-1, critical in transcriptional regulation of genes whose products mediate angiogenesis and hypoxic adaptation. HIF-1α is overexpressed in human cancers, predominately through defects in degradation pathway. Mammalian lipoxygenases (LOXs) are key mediators of arachidonic acid metabolism relevant to carcinogenesis. 15-LOX-1 has recently been demonstrated to be down-regulated in several common malignant tumors, and the degree of its down-regulation is reversely correlated to advanced tumor stages. Our prior studies have shown that inhibiting 15-LOX-1 increases HIF-1α level and HIF-1 transcriptional activity (2002 AACR) while mechanistic details remain elusive.
Design: Prostate cancer and colon cancer cell lines and human tissue microarray were employed. 15-LOX-1 expression vector was subcloned so as to manipulate its enzymatic activity. Stable or transient transfection plus luciferase assays, immunoprecipitation, HIF-1α ubiquitination assay, and immunohistochemistry were utilized in the study.
Results: Here, we report that 15-LOX-1 promotes HIF-1α ubiquitination and degradation, depending on the classic Pro^{564}/hydroxylation/26S proteasome system under normoxia. Both enzymatic activity and intracellular membrane binding function of 15-LOX-1 are required to degrade HIF-1α. The enhanced HIF-1α degradation by 15-LOX-1 overexpression is not abolished even if proteasomal degradation is inhibited by hypoxia or $CoCl_2$. No physical association between immunoprecipitated HIF-1α and 15-LOX-1 occurs, which further supports that enzymatic products of 15-LOX-1 likely mediate the decrease in HIF-1α. In addition, induction of endogenous 15-LOX-1 simultaneously reduces hypoxia-induced HIF-1α accumulation in a dose dependent pattern. Finally, 15-LOX-1 down-regulation was demonstrated by immunohistochemical studies in breast or other common malignancies compared to their benign counterparts.
Conclusions: Our findings provide a novel mechanism for the HIF-1α regulation that combines oxygen dependent and oxygen insensitive actions. This is the first evidence demonstrating that a lipoxygenase involves HIF-1α regulation. Lowered 15-LOX-1 is probably one of the many reasons of HIF-1α overexpression in human cancers, which contributes to diseases progression.

1754 Significance of Loss of Heterozygosities in Predicting Sentinel Lymph Node Metastasis of Breast Invasive Ductal Carcinoma

B Zhu, SD Finkelstein, R Saad, JF Silverman, X Lin. Northwestern University, Chicago, IL; RedPath Integrated Pathology, Inc., Pittsburgh, PA; Allegheny General Hospital, Pittsburgh, PA.
Background: Sentinel lymph node (SLN) metastasis of breast invasive ductal cancer (BIDC) is one of the main criteria determining stage that is the strongest predictor of disease aggressiveness and survival, and determining the need for axillary resection and additional therapy. We studied SLN metastasis using a combined histopathologic/molecular approach to gain insights into the pathobiology implications.
Design: Fourteen BIDC patients with positive SLN and 19 with negative SLN were retrieved. Analysis of 17 polymorphic microsatellite repeat markers targeting 1p34-36, 3p24-26, 5q23, 9p21, 10q23, 17p13, 17q12, 17q21, 21q22, and 22q13 was performed in DNA isolated from primary tumors and metastatic tumors.
Results: BIDCs with SLN metastasis showed larger size (p=0.004) and higher nuclear grade (P=0.047) than those with negative SLN, which correlated with higher fractional mutation rate (FMR) of the primary tumor and shared FMR by the primary and SLN tumors. SLN metastasis was not related with expression of estrogen receptor, progesterone receptor, and Her2/neu, and did not correlate with higher FMR. However, higher FMR was related to higher percentage of positive SLNs. Tumor size is not necessarily a strong marker for the prediction of aggressiveness and metastasis of BDC, indicting that some smaller BIDCs arise intrinsically as an aggressive malignancy with metastatic disease. LOHs at 1p34-36, 3p24-26, 9p21, 10q23, 17p13, 17q12, 21q22 and 22q13 may play an important role in the development and aggressiveness of BIDC. LOHs at 1p34-36, 17p13 and 22q13 may play an important role in metastasis. None of the LOHs were shared by all the tumors, suggesting that BIDC develops using various pathways that have unique and personalized patterns of mutational changes.
Conclusions: Detection of LOH is useful in studying oncogenesis and predicting aggressiveness and metastasis of BIDC.

Pediatrics

1755 Morphoproteomic Profiling of Choroid Plexus Carcinoma Reveals Constitutive Activation of the mTOR and ERK Pathways with Cell Cycle Progression

RE Brown, J Buryanek, JE Wolff. University of Texas-Medical School, Houston, TX; University of Texas-M.D.Anderson, Houston, TX.
Background: Choroid plexus carcinoma (CPC) is a rare pediatric malignancy with a poor prognosis despite conventional therapies. Understanding its molecular biology should provide insight into targeted therapeutic options. To this end, we performed morphoproteomic profiling on two such cases.
Design: Sections of an original and recurrent CPC, were available for analysis. Immunohistochemical probes were applied to detect the following: 1. phosphorylated (p)-mammalian target of rapamycin (mTOR) [Ser 2448]; p-Akt (Ser 473); p-p70S6K (Thr 389); and p-extracellular signal-regulated kinase (ERK) 1/2 (Thr 202/Tyr 204); and 2. cell cycle-related proteins to include nuclear Ki-67(G1, S, G2 and M phases), S-phase kinase-associated protein (Skp)2 (promotes G1 to S), p53 (wild type regulates, mutant form permissive in G1 to S) and topoisomerase II alpha (facilitates S to G2/M). Quantification of the nuclear percentages was carried out, whenever possible, by an automated cellular imaging system (ACIS). Mitotic indices were calculated as an average of mitotic figures in the most mitotically active regions per sets of ten high power fields (h.p.f.'s).
Results: Constitutive activation of the Akt/mTOR and ras/Raf kinase/ERK pathways is evident in both cases with predominantly plasmalemmal and cytoplasmic expressions of p-Akt (Ser 473) and p-mTOR (Ser 2448), favoring the mTORC1 pathway, and with nuclear expression of p-p70S6K (Thr 389) and nuclear p-ERK 1 / 2 (Thr 202/Tyr 204). Correlative cell cycle progression was noted with mean nuclear expressions in each of the cases as follows: Ki-67 at 14.0 and 11.6%, Skp2 at ~20% (visual quantification) and 7.8% and 28 and 27 mitotic figures per 10 h.p.f.'s, respectively. Nuclear topoisomerase II alpha at 96 and 52.1% and p53 at ~30 and 63% (probably mutant form) were noted.
Conclusions: Morphorproteomic profiling reveals constitutive activation of the Akt/mTOR and ras /Raf kinase/ERK pathways, which appears to be the first report of its kind in CPC. Such activation coincides with downstream signal transduction from insulin-like growth factor (IGF) II/IGF-type 1 receptor and platelet-derived growth factor receptor, previously reported in CPC. Moreover, it accords with the cell cycle progression and provides opportunities to apply combinatorial therapies to target the mTORC1 pathway, cell cycle progression and topoisomerase II alpha in CPC.

1756 Sorafenib Down Regulates Akt and STAT3 Survival Pathways and Induces Apoptosis in a Human Neuroblastoma Cell Line

H Chai, A Luo, P Weerasinghe, RE Brown. University of Texas- Medical School, Houston, TX.
Background: Neuroblastoma ranks second among solid tumors in children, and its tumorigenicity is enhanced by the expression of survival pathways such as Akt, Nuclear Factor (NF)-kappaB and signal transducer and activator of transcription (STAT)3 and the expression of the anti-apoptotoic protein, Mcl-1. Sorafenib is a multi-kinase inhibitor that also inhibits STAT3 signaling and induces apoptosis in association with downregulation of Mcl-1. In this study, we examine the efficacy of sorafenib on a human neuroblastoma cell line and also investigate its possible mechanisms.
Design: A neuroblastoma cell line, SK-N-AS, was purchased from ATCC. After reaching 50-60% confluence, cells were treated with various concentrations of sorafenib (0, 0.1, 1, 5, 10 and 20 μM) for different period of times (2, 6, 24, 48 and 72 hours). The cell viability was determined by MTT colorimetric assay. The apoptotic responses were